Ministry of Higher Education and
Scientific Research/ Baghdad University
Institute of Laser for Postgraduate Studies

Fast Optical Fiber Sensor for Temperature Elevation Detection during Laser Cavity Preparation

A thesis

Submitted to the Institute of Laser for Postgraduate studies, University of Baghdad in partial fulfillment of the requirements for the degree of Master of Science in Laser / dentistry

By

Zahraa Jabier Naeem

B.D.S.

Supervisor

Prof. Dr. Abdul Hadi Al Janabi

2021 AB **1443 AH**

Certification

I certify that this thesis was prepared under my supervision at the Institute of Laser for Postgraduate Studies, University of Baghdad, as a partial fulfillment of requirements for the degree of "Master of Science in Laser / dentistry ".

Signature:

Name: **Dr. Abdul Hadi Al-Janabi**

Title: **Professor**

Address: Institute of Laser for Postgraduate studies,

University of Baghdad.

Date: / / 2021

(Supervisor)

In view of the available recommendation, I forward this thesis for debate by Examining Committee.

Signature:

Name: Dr. Hanan Jaafar Taher

Title: Head of the Scientific Committee.

Address: Institute of Laser for Postgraduate studies,

University of Baghdad.

Date: / / 2021

Acknowledgment

First of all, I would like to thank **Allah** for inspiring me with the strength, patience and willingness to perform this work.

I wish to express my sincere appreciation to my supervisor **Prof. Dr. Abdul Hadi AL Janabi**, whom I was fortunate to be under his supervision for his excellent supervision, I am deeply indebted to his for his patience, advice, and scientific support.

I would like to express my gratitude and highest appreciation to the *Dean of the Laser Institute for Postgraduate Studies* **Prof. Dr. Hussein A. Jawad**, for his kindness, patience, and encouragement.

Also, I am so fortunate for the advice and encouragement of **Dr. Ansam Majid**, for her scientific advisement and help.

I also thank **Dr. Rawaa A. Faris**, for helping me in my thesis.

I wish to express my grateful respect and admiration for my **parents and my small family** that supported me with care, patience and encouragement, whom without their love, care, and patience, I am nothing and worthless.

Finally, the support from my husband **Hussein Ali Dosh**, as always, the first supporter; my deepest gratitude goes to him for help, support, and care in my present work and in the whole of my life….

Thank to them all

ABSTRACT

Objective: A rise in temperature can happen as a result of heat buildup during the cavity preparation of dental hard tissues using laser beam. An innovative measuring modality based on fiber sensor for measurement instantaneously of the heat elevation in enamel and dentin dental hard tissues is applied. The impact of Nd:YAG laser with 1064 nm wavelength as well as Er,Cr:YSGG of 2780 nm wavelength on the enamel and dentin dental tissues have been tested.

Materials and Methods: A number of 110 dental hard tissue samples taken of both enamel and dentin of different layer thicknesses were prepared. The impacts of both aforementioned laser wavelengths in terms of the thermal negative affect upon dental pulp while laser cavity preparation have been tested. Firstly, half of these dental hard tissues have been treated with the near infrared Q-switched Nd:YAG laser (λ =1.06 μm) of a pulse duration of 9 ns, 10 Hz repetition rate, and total energy of 850 mJ and an average power of ~8.5 W. Those samples were irradiated using heat conductive paste as an interface medium without any cooling or water spray. After that, the influence of Er,Cr:YSGG laser (λ =2.7μm) with pulse duration of 60μs, energy of 260 mJ, repetition rate of 15 HZ, fiber tip diameter of 600 μm and power of 4 W has been investigated with a rate of 50% water and 80% air spray.

For the instantaneous and quick temperature elevation measurement, a novel fiber optic sensor with a balloon like shape has been designed and constructed. The easily adapted fiber optic sensor attached to the back of both the enamel and dentin samples relies on Mach-Zehnder interferometer principle. The above sensor, that has been used, possesses a quick response time of ~1 ms, a speedy recovery time of 2.73 ms, as well as a high resistivity at around 1.975 nm/^{0}C. Data were statistically analyzed by one-way and two-way analysis of variance (ANOVA) at the 95% confidence level and compared by Tukey post hoc test (a = 0.05)

Results: Two different types of lasers (Nd:YAG and Er,Cr:YSGG) have been used to perform the in-vitro experiments. As the pulpal vitality safe limit will determine the used laser parameters, Nd:YAG laser cavity preparation without water cooling showed higher temperature elevation than Er,Cr:YSGG laser in three subgroups (enamel 1mm, enamel 2mm and enamel 2mm thickness). While the lowest temperature values were observed in (dentin 3mm) subgroup.

Nevertheless, the applied laser beams were controlled fully to avoid the unwanted temperature elevation via the used optical fiber sensor. The sensor due to its unique characteristics help much in giving an in time useful response to keep pulpal vitality.

Conclusions: The combination of highly efficient laser for cavity preparation and fast response time, easily adapted fiber sensor will provide a potential platform to avoid pulpal necrosis through laser dental ablation process.

List of Contents

List of Tables

List of figures

List of Abbreviations

Abbreviations	***Term***
α	Coefficient of absorption
AFM	Atomic force microscopy
ANOVA	Analysis of variance
$Ca_{10}(PO_4)_6OH_2$	Hydroxyapatite crystal
DEJ	Dentino enamel Junction
DRMs	Dental restorative materials
EDX	Energy dispersive x-ray
FDA	Food and Drug Administration
FESEM	Field emission scanning microscopy
FTIR	Fourier transform infrared spectroscopy
HS	Highly significant
HSHPs	High speed hand pieces

IPTR	Intra pulpal temperature rise
J/cm^2	Joule per square centimeter (unit of energy density)
L	Penetration depth
LF technique	Laser fluorescence technique
LITT	Laser Interstitial Thermal Thermotherapy
LSHP	Low speed hand pieces
LSO	Laser safety officer
mW	Mili Watt
MZI	Mach-Zehnder interferometer
Nd:YVO4	Neodymium-doped yttrium orthovanadate
NIR	Near infrared
NS	Non-significant
OdP	Odontoplastic processes
OFSs	Optical fiber sensors
OSA	Optical spectrum analyzer
R^2	Linear regression coefficient
RH sensor	Relative humidity sensor
S	Significant
SD	Standard deviation
SEM	Scanning electron microscope
SE	Standard error
SMF	Single mode fiber
SSP	Super short pulse
USPL	Ultrashort pulsed laser
VLP	Very long pulse
VSP	Variable square pulse
W/cm^2	Watt per square centimeter (unit of power density)

Chapter One

Introduction and Basic Concepts

CHAPTER ONE

Introduction and Basic Concepts

1-1 General introduction and motivation:

Previous years witnessed an expansion in the area of minimally invasive procedures built on thermal therapies for instance: laser ablation, high intensity focused ultrasound ablation, radiofrequency ablation, microwave ablation, and cryo-ablation [1,2]. These procedures cause a localized temperature increase or decrease, which can cause physical damage or even irreversible insult to the patient [3,4]. So, although working temperature is restricted to a relatively specific scale, temperature control is correlated directly to the performance improvement of all these therapy procedures [5]. A detailed measurement of tissue temperature can be particularly useful for improving outcomes and controlling the delivered energy environment during rehabilitation.

Notably, for therapeutic and experimental uses of lasers, precise laser irradiation parameter [6] such as repetition rate, wavelength, energy density, average power, peak power, intensity, as well as pulse duration are tremendously crucial and must be selected carefully in an attempt to avoid morphological damage, for instance, surface charring or cracking, that could bring in esthetic, structural hurts, as well as post-operative complaint. In addition, the pulp as well as periodontal tissues' viability is protected. The target tissue's optical properties, such as absorption and scattering coefficients, have a major impact on the overall heat within it. Besides that, heat transfer is influenced by thermal tissue properties for instance thermal diffusivity, thermal conductivity [7,8].

To improve safety and accurate monitoring, temperature sensor devices must have a real-response time, highly sensitive, biocompatible and precision deprived of causing any harm to the host [9,10].

The biomedical sensor related to body temperature should meet certain criteria in specific configurations, including non-toxic sensing medium, ease of sweeping and sterilization, and insensitivity to many further physical parameters excluding temperature [11,12]. Traditional thermometers were used to calculate temperatures for a long time, but they have inaccuracies in calculation and/or a long response time [13]. Health monitoring sensor systems based on fiber devices consume a lot of attention as potential innovations thanks to the advancement of human-approachable smart resources [2,14]. Fiber optics as such an effective temperature sensing feature is an appealing thermometric tool because it can provide accurate description, versatility, small size, simplicity, non-harmful, corrosion-resistant, extremely resistant to electromagnetic interference, as well as short response time in the sub to several milliseconds scale [9,15-18]. Furthermore, these sensors can perform distributed, sort of semi-distributed, and several points measurements, allowing for temperature measurement in different points of tissue by inserting a small sensor component with a simple design [2,19]. These advantages make optical fiber sensor technology super spectacular for temperature observing through thermal treatments. The interference phenomenon was the basic theory used to establish responsiveness in optical fiber sensors. The sensing head's balloon-like geometry has a number of distinct advantages, including low cost, ease of fabrication, high sensitivity, fast response time, and high resolution [20,21].

In both everyday life and therapeutic clinical dentistry, transmission of heat in human tooth is a typical occurrence [22-25]. With progress in recent current dentistry, tools having an elevated energy output (for example, dental lasers) [26,27], light polymerization units [28-30] as well as high speed hand pieces [31,32] have been commonly used in dental procedures. Table (1-1) lists the currently available therapies and the corresponding intrapulpal temperature rise.

Table (1-1): Typical thermal therapies and relative intrapulpal temperature rise (IPTR) [33]

Laser Treatment	**Temperature rise (◦C)**
Laser assisted tooth ablation	2.3–24.7
Laser assisted caries prevention	1.2–4.0
xBleaching (without light/laser assisted	0.1–1.1
Bleaching (with light/laser assisted)	1.1–16.0
Polymerization of dental restorative materials (DRMs)	2.9–7.8
HSHPs cavity preparation (without water, high load)	16.4–19.7
HSHPs cavity preparation (without water, low load)	7.1–9.5
HSHPs cavity preparation (with water, high load)	2.2–5.9
HSHPs cavity preparation (with water, low load)	−1.8 (drop in temperature) to 5.0

1-2 Structure of human tooth

A living human tooth is indeed multilayered structure containing enamel, dentine, cementum, as well as dental pulp [34] with multifaceted geometry. The enamel is really mineralized layer that is 96% mineral and 4% water and organic components. The dentine is often mineralized layer of connective tissue alongside a collagenous protein organic pattern [35,36], by weight, it is made up of 70% inorganic components, 20% organic elements, and 10% aqueous fluid. Dentinal tubules radiate from pulp chamber to the exterior cementum or else dentino-enamel junction (DEJ) [36]; as shown in figure (1-1). A human tooth sensory tissue as well. The pulp is indeed soft connective tissue that contains nerve fibers ranging in diameters between 1 and 10 mm. Dentinal tubules also have included sensory nerve endings [37], which infiltrate just about 100–150 μm within the tubules from walls of pulp cavity [38]. Those pulpal nerve endings are crucial in the detection of temperature stimuli. In terms of development, structure, and functionality, the dentine and the pulp are very similar [39]. Despite the fact that pulp and dentin are anatomically and chemically distinct [36], they work as a single unit, known as "dentine-pulp complex" [39].

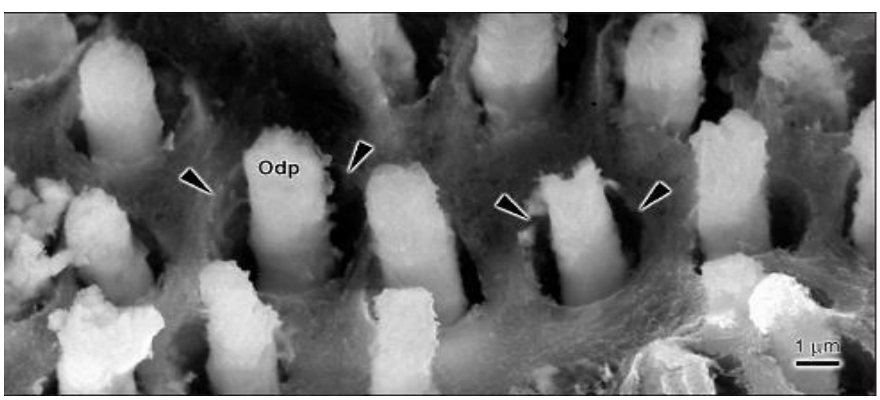

Fig. (1-1): Image from scanning electron microscope showing Odontoblast processes run in dentinal tubules [40].

1-3 Heat generation in human tooth

In both daily life, heat transmission happens in teeth. Teeth are exposed to wide range of temperatures (from –5 to 76.3 ^{0}C) throughout their daily lives [41]. Table (1-2) shows intraoral temperatures estimated in vivo besides calculated ultimate temperature during ingesting of hot brew and diet.

Excessive heating of both enamel and dentine throughout laser-tooth interactions, however, is a big problem, as it promotes carbonization, tissue charring, melting, and cracking for both tooth enamel and dentin, along with pulp necrosis. Dental restorative processes are used to decrease the polymerization periods of resin composite and minimize its polymerization shrinkage. During these processes, teeth are exposed to the radiation of LUPs (e.g., halogen polymerization lamps or semiconductor diode light) and experience substantial temperature increase of 10–18 ◦C within the resin and adjacent tooth [42,43], 7.5–29 ^{0}C at DEJ [44], as well as 2–9 ^{0}C at pulpal chamber wall [44].

Treatments with HSHPs (high speed handpieces) are performed in dental clinics for applications such as cavity preparation. Heat is generated by friction between the machinery (e.g., driller) and tooth, resulting in intra pulpal temperature rise [31,32,45]. This temperature growth relies on pressure and speed of the hand pieces [33] in addition to the cooling techniques used [31].

Despite the fact that both enamel and dentin being predominantly made up of hydroxyapatite crystals ($Ca_{10}(PO_4)_6OH_2$), which operate as insulation material, thermal as well as non-thermal stimulation given to dental structures may cause pulpal reactions [31]. Unlike heat conduction in engineering materials [46], the thermal performance of teeth is mostly a heat conduction mechanism linked with dental physiological procedures (e.g., dentinal fluid flow, pulpal blood stream) [42]. The thermophysical properties of teeth vary between different layers (e.g., enamel and dentine) [43] and depend on their microstructures. For instance, the thermal conductivity of human dentin decreases with increasing volume fraction of dentine tubules [47]. The flow of dentinal fluid in the dentine tubules upon heating (or cooling) can also enhance heat generation within the pulp. Furthermore, while the intra pupal temperature goes over 42°C, the rate of pulpal blood flow increases, and once the temperature drops, it decreases [42]. The perfused blood plays an important role in the thermoregulation of pulpal soft tissue, working as a heat sink under heating and as a heating source when subjected to cooling.

Table (1-2): Intraoral temperatures estimated in vivo and calculated ultimate temperature during ingesting of hot brew and diet [48].

Temperature (◦C)	**Hot brew**	**Hot diet**
Highest a*	76.3	53.6
Mean maximum b**	46.4	41.6
Calculated extreme c***	61.4	50.2

*a highest temperature calculated in one volunteer among the lower incisors.

**b Mean maximum temperature ± standard deviation documented by each electrode for the whole volunteers.

***c Calculated extreme temperature got by adding binary standard deviations for the mean maximum temperature calculated in vivo

1-3-1 Response of pulp and supporting tissue to thermal irritation

Even though external stressors for example 'thermal irritation'- could harm pulp tissue and produce alterations in it, a straight link connecting the measured temperature and the actual tissue harm is not always discovered [49]. Furthermore, determining the origin of pulpitis in clinical conditions is challenging since this elimination of a tooth structure is followed by physical injury and also thermal discomfort [50].

Small temperature variations (from 37 to 42 ^{0}C) can be tolerated by the dental pulp throughout short periods of time (30 to 60 s) before causing permanent harm. There was around 60-70% irreversible pulpitis whenever the intra pulpal temperature increased to 11.1°C for 10 s [50]. Transitory temperature growths of around 8.9-14.7 ^{0}C (mean, 11.2 ^{0}C) did not induce pulp injury in further recent in vivo research on teeth of human [51]. Under many circumstances, the pulp's microcirculation carries heat away from the pulp to many other areas of the body, where it can be easily dissipated. Extreme temperature increases or prolonged resistant to high temperatures, on the other hand, will result in pulpal alterations [52].

For dental applications, prolonged thermal exposure periods must be avoided to guard the dental pulp [52] numerous alterations can happen by heat production, for example, tissue burning, postoperative sensitivity, and pulp necrosis. Pulpal temperature increases with Er:YAG laser and high-speed handpieces. Zach and Cohen reported 15% irreversible pulpal necrosis after a 5.6˚C increase of intrapulpal temperature and up to 60% necrosis after an 11 ˚C rise [50]. The irradiated dentin's morphology has been described as having an uneven surface with exposed dentinal tubules as well as an absence of smear layer [53,54].

As a result, it's also possible that speed as well as time of thermal motivation, including magnitude of rise in temperature, have a part in pulp damage, and even that slow temperature increases could boost the threshold temperature elevation above 5.6 ^{0}C. Nevertheless, remaining dentin thickness is yet another crucial component impacting intra pulpal temperature increase, and in cases involving teeth preparing as well as light curing for composite resin, when the leftover dentin is thinner, this could create a more dangerous condition [49].

However, due to heat dissipation via pulpal, periodontal, in addition to osseous circulation, as well as improvements in pulp circulation by neurological reflex, it may be hypothesized that intra pulpal temperature rises are lower in true clinical conditions than invitro conditions [51,55]. Temperature rises on the outside of root surface during some endodontic operations, may create a risk of injury to the cementum of the root, periodontal ligament, as well as alveolar bone [56].

Several studies have suggested a temperature threshold which can harm tooth-supporting tissues [56]. Since alkaline phosphatase is lysed at this temperature, 19°C was thought to be the critical temperature rise for alveolar bone [56]. The recovery of bone tissue after heat damage occurred via the production of connective tissue rather than hard-tissue creation, implying that threshold rise in a temperature indicated for bone injury was 10 ^{0}C. Sauk et al. found that even though a lower threshold rise in the temperature, claiming that whenever the temperature of periodontal ligament increased by 6 ^{0}C, protein denaturation occurred, resulting in ankyloses as well as alveolar bone resorption [57]. Although a precise temperature was not stated in some in vivo experiments, when heat stimulation was applied to the endodontic sidewall, localized necrosis, bone-resorption, as well as ankyloses were observed on periodontal ligament [58,59]. As a result, supporting tissue of the tooth threshold rise in temperature of 10 ^{0}C is higher than the pulp's of 5.6 ^{0}C. The 'burn reaction,' that involves blister development, death of ectopic odontoblasts, coagulation of protoplasm, enlargement of fluid content of dentinal tubules, and also an increase in inward flow, seems to be the method of pulp necrosis caused by thermal trauma. This damages the internal blood vessels, causing vascular damage and, eventually, pulp necrosis [50].

Even though the in-vitro testing procedure, which used a thermal resistor for stimulation and measured intra pulpal temperature, was similar to Zach and Cohen's earlier work, there were differences in the velocity and length of the thermal stimulation. The impulse's length was determined by a symptomatic criterion, in other words, it was kept for around 30 s just after patient stated that the stimulation had become uncomfortable. A progressive temperature rise over roughly 200 s was replicated, and thus the tooth was assessed clinically and histologically, much like in real life.

1-3-2 Thermal irritation through tooth preparation via high- coupled with low-torque hand pieces

Because dental operations typically use hand pieces to remove tooth structures, both high-and also low-speed hand pieces are by far the most commonly employed. Temperature rises of 1.8 ^{0}C, 1.4 ^{0}C, as well as 0.7 ^{0}C were observed with low-speed hand piece (LSHP), high-speed hand piece (HSHP), then laser, accordingly, with an in-vitro research with a 0.5 mm remaining dentin thickness [60].

Although there were no substantial differences between both the LSHP and HSHP groups, there was even a significant finding with a lowest temperature rises in the laser group. In an investigation done by Srimaneepong et al., [61] founds that the thinner remaining dentin thickness in addition to the superior laser power, the further the temperature growth. A lesser temperature increase was noted while utilizing a laser to remove normal tooth structure in comparison to when working with HSHP [61]. Watson et al. founds the same results when he utilized a water spray cooling accompanying HSHP and LSHP to eliminate tooth structure, and they discovered a surprise drop in intrapulpal temperature [62]. The kind of burs employed could alter the rise in temperature; diamond bur cause bigger temperature rise than carbide bur, but again the effect was not substantial due to water cooling [62]. Because the reported temperature rise is very minimal, it is doubtful that tooth preparation employing HSHP or even LSHP with water cooling produces pulp damage. Dentists do occasionally use a LSHP device with no water spray to remove deep caries. When cavities are prepared without cooling, the intra pulpal elevation in temperature may exceed Zach and Cohen's proposed threshold rise in temperature of 5.6 ^{0}C, causing pulp damage [63]. The highest intra pulpal temperature measured for teeth treated without any water spray was 24.7 ^{0}C, compared to 3.9 ^{0}C for the teeth treated with water spray, as stated by Attrill et al [63]. Another study found that whenever a LSHP had been used with no cooling, the intra pulpal temperature rises to critical temperature of 5.6 ^{0}C in only 20 s just after bur makes contact with the tooth structure, while when a LSHP has been used with water spray, intra pulpal temperature reduction was noticed [64]. To summarize, it is vital to utilize a hand piece with water spray cooling to reduce thermal injury to the pulp throughout tooth preparation, and when it is used in a dried cut, the burr contact time should be limited to 20 s.

1-4 Laser-tissue interaction

Laser light energy can interact along with the tissue into four diverse ways, dependent on optical tissue properties. The laser light could be reflected, absorbed, scattered, or transmitted once it hits a tissue surface [65], as shown in figure (1-2). The fractional intensity which goes into those procedures is governed by the tissue's optical properties, for instance: absorption coefficients, scattering coefficients, reflectivity, as well as particle size [66], in addition to the laser parameters for example: pulse duration, wavelength, operation mode and energy [67].

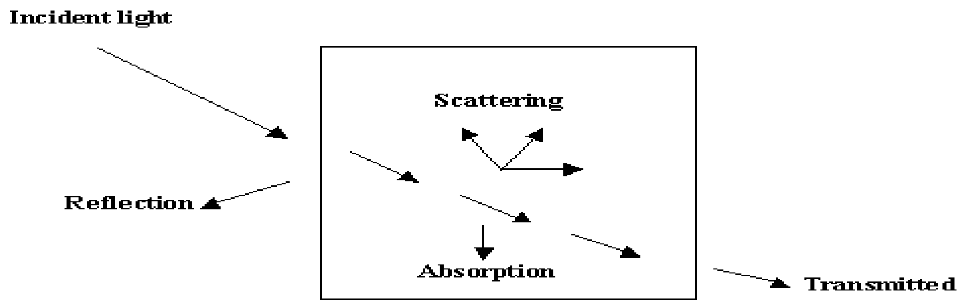

Fig. (1-2): Reflected- refracted- scattered-absorbed and transmitted laser light when hits a tissue surface [66].

The other laser parameter is the laser light’s absorption into biological tissue, which is particularly relevant to therapy. Absorption happens when the energy of an incident photon harmonizes the energy difference between two molecule’s levels into biological tissues. Laser light’s electromagnetic energy would be converted to different energy forms after it has been absorbed by tissue. Photon interactions with tissue molecules can cause structural tissue alterations in this situation [68]. Some details on laser interaction with biological tissues are explained in following sub-sections.

1-4-1 Reflection:

This is merely the laser being redirected away from the target tissue, without any effect on it. Since the energy redirected toward an unintentional target, for instance the eyes, this redirection can be harmful. This is a key safety problem for laser operation [69].

1-4-2 Absorption:

The intensity of an electromagnetic wave incident on the tissue is weakened as it passes through a material during absorption. Absorption occurs when light energy is partially converted into thermal motion or specific vibrations of absorbing material's molecules. If a substance lowers intensity of whole spectrum’s wavelengths via similar percentage, it is thought to have general absorption. Such substance will seem grey to our eyes when exposed to visible light. Selective absorption, from the other hand, occurs when particular wavelengths are absorbed over others. The capacity of any medium to absorb electromagnetic radiation is determined by a variety of factors, including electronic constitution of its atoms and molecules, wavelength of electromagnetic radiation, approximate thickness of absorbing layer, as well as internal parameters such as temperature or absorbing material concentration. Biological tissues absorption (figure 1-3), which is mainly caused by either water molecules or macromolecules such as proteins and pigments. Whereas absorption in the IR region of the spectrum can be primarily attributed to water molecules, proteins as well as pigments mainly absorb in the UV and visible range of the spectrum. Since neither macromolecules nor water strongly absorb in the near IR a “therapeutic window” is delineated between roughly 600 nm and 1200 nm. In this spectral range, radiation penetrates biological tissues at a lower loss, thus enabling treatment of deeper tissue structures [70].

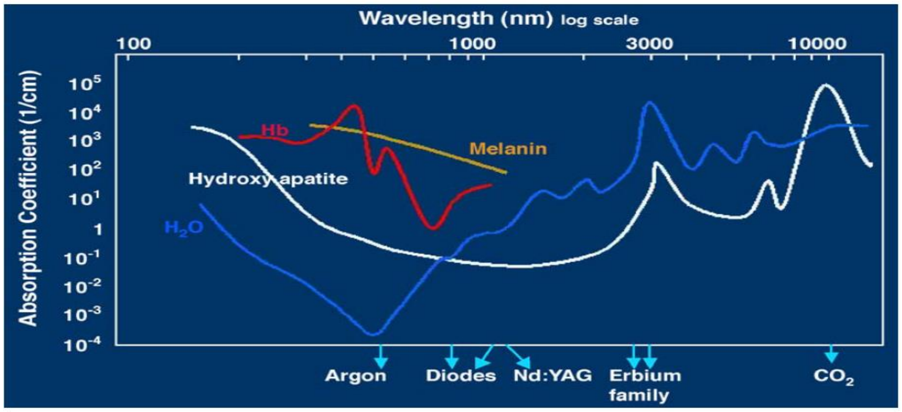

Fig. (1-3): Estimated absorption curves of various dental Compounds thru various wavelengths of lasers used in dental field [71].

1-4-3 Transmission:

The direct transmission of laser light through tissue without any influence on the target tissue. The laser light wavelength has a significant impact on this effect. Just non-reflected and non-absorbed photons, as well as forward scattered photons, would pass through the tissue [69].

1-4-4 Scattering:

Altering the path of photons inside the tissue, based on whether portion of incoming photon energy is being transformed through scattering procedure, the elastic as well as inelastic scattering are separated. Rayleigh scattering is indeed a type of elastic scattering. Rayleigh scattering is indeed elastic scattering, with the single requirement that scattering particles be smaller compared with wavelength of the incident radiation. Brillouin scattering is really a valuable type of inelastic scattering. It is caused by acoustic waves traveling across a material, causing refractive index inhomogeneity. Brillouin scattering of light to higher (or lower) frequencies occurs, because scattering particles are moving toward (or away from) the light source. Rayleigh scattering is no longer applicable, and a new form of scattering known as Mie scattering takes its place. The philosophy of Mie scattering is somewhat complicated, so we won't go through it here. It should be noted, nevertheless, the Mie scattering as well as Rayleigh scattering differ in two key ways. Firstly, compared with Rayleigh scattering Mie scattering has a reduced wavelength dependency. Secondly, Mie scattering occurs mostly a forward direction, while Rayleigh scattering occurs in both the forward as well as backward directions [70].

1-5 Laser interaction mechanisms

Different interaction mechanisms might take place whenever laser light is applied to biological tissues because of specific tissue properties and laser parameters.

1-5-1 Wavelength Dependent Mechanisms

1-5-1-1 Photochemical Interaction Mechanism

The photochemical interaction processes are based on actual evidence that light could cause chemical effects as well as reactions within macromolecules and tissues. Photochemical interactions take place at very low power densities (typically 1 W/cm^2) and long exposure times ranging from seconds to continuous wave. The photochemical interaction processes have been used in a variety of applications [70].

1-5-1-1-1 Photodynamic Therapy

Exogenous chromospheres, also known as photosensitizes, mediate the photodynamic treatment reaction. In this case, the light is used for activation of molecules or drugs by a specific wavelength of the laser light. The molecule is transformed into toxic compound, often involving oxygen-free radical that can cause cellular death through destruction of the DNA molecule [70].

1-5-1-1-2 Biostimulation

This process is believed to occur at low irradiance or extremely low laser power. It is related to enhancing certain metabolic pathways in the living cells, for example, healing of skin lesions and relief of pain. According to Karu (1987), local wound healing effects with helium-neon or diode lasers may be explained by the action of low intensity light on cell proliferation. In the area of such injuries, conditions are usually created preventing proliferation such as low oxygen concentration or pH. The exposure to red or near infrared light might thus serve as a stimulus to increase cell proliferation [72].

1-5-1-1-3 Photoablation therapy

Srinivasan *et*. and Mayne Banton were the first to identify photoablation (1982). They named it ablative photodecomposition, which means that when a substance is subjected to high-intensity laser irradiation, it decomposes. It occurs whenever laser light's energetic photons disintegrate molecules via breaking chemical bonds. In this type of reaction, Photoablation is because of "***volume stress***" according to bond breaking. Tissue removal is done in a highly clean and precise manner, with no evidence of thermal insult for example coagulation or vaporization. At pulse duration of laser in the nanosecond band, average threshold values for such kind of interaction are 10^7 to 10^8 W/cm^2. The accuracy of the etching procedure and the absence of heat damage to neighboring tissues are the key advantages of such an ablation technology [70].

1-5-1-2 Photothermal Interaction Mechanism

The term thermal interaction stands for a large group of interaction types, where the increase in local temperature is the significant parameter change. Thermal effects can be induced by either CW or pulsed laser radiation. Temperature certainly is the governing parameter of all thermal laser- tissue interactions. The spatial extent and degree of tissue damage primarily depend on magnitude, exposure time, and placement of deposited heat inside the tissue. Deposition of laser energy is a function of laser parameter: such as wavelength, power density, exposure time, spot size, and repetition rate, optical tissue parameter and thermal tissue parameter. In biological tissue, absorption is mainly due to the presence of free water molecules, proteins, pigments, and other macromolecules. The thermal effects of laser radiation and the biological effect are demonstrated in table (1-3).

Table (1-3): Thermal effects of laser radiation [70].

Temperature	**Biological effect**
37 ^{0}C	Normal
45 ^{0}C	Hyperthermia
50 ^{0}C	Reduction in enzyme activity, cell immobility
60 ^{0}C	Denaturation of proteins and collagen, coagulation
80 ^{0}C	Increase permeability of membranes
100 ^{0}C	Vaporization, thermal decomposition (ablation)
>100 ^{0}C	Carbonization
> 300 ^{0}C	Melting

1-5-2 Wavelength Independent Mechanisms

When employing power densities beyond 10^{11} W/cm² in solids as well as in fluids or else 10^{14} W/cm² into air, multiphoton ionization of molecules and atoms may happen when the pulse duration would be into the picosecond to femtosecond region, resulting in a phenomenon known as optical breakdown. Generation of plasma and shock waves are the two physical processes related with optical breakdown. Cavitation and jet formation can happen when breakdown takes place within soft tissues or fluids.

The important feature of the optical breakdown is that it renders possible an energy deposition not only in pigmented tissue, but also in nominally weakly absorbing media. This means that the interaction does not depend on the wavelength. By means of plasma induced ablation, very clean and well defined removal of tissue without evidence of thermal or mechanical damage can be achieved when choosing appropriate laser parameters.

With picosecond as well as femtosecond pulses, large peak intensities can be achieved with much lower pulse energies. Optical breakdown could still be accomplished with these extremely small pulse durations while drastically decreasing plasma energy and, hence, disruptive effects. Mechanical forces break the tissue throughout photo disruption. Plasma-induced ablation, on the other hand, is spatially limited to breakdown region. Even at the incredibly high thresholds, optical breakdown has always been accompanied with shock wave production for nanosecond pulses [70,73]. The laser tissue communication mechanisms are demonstrated in figure (1-4).

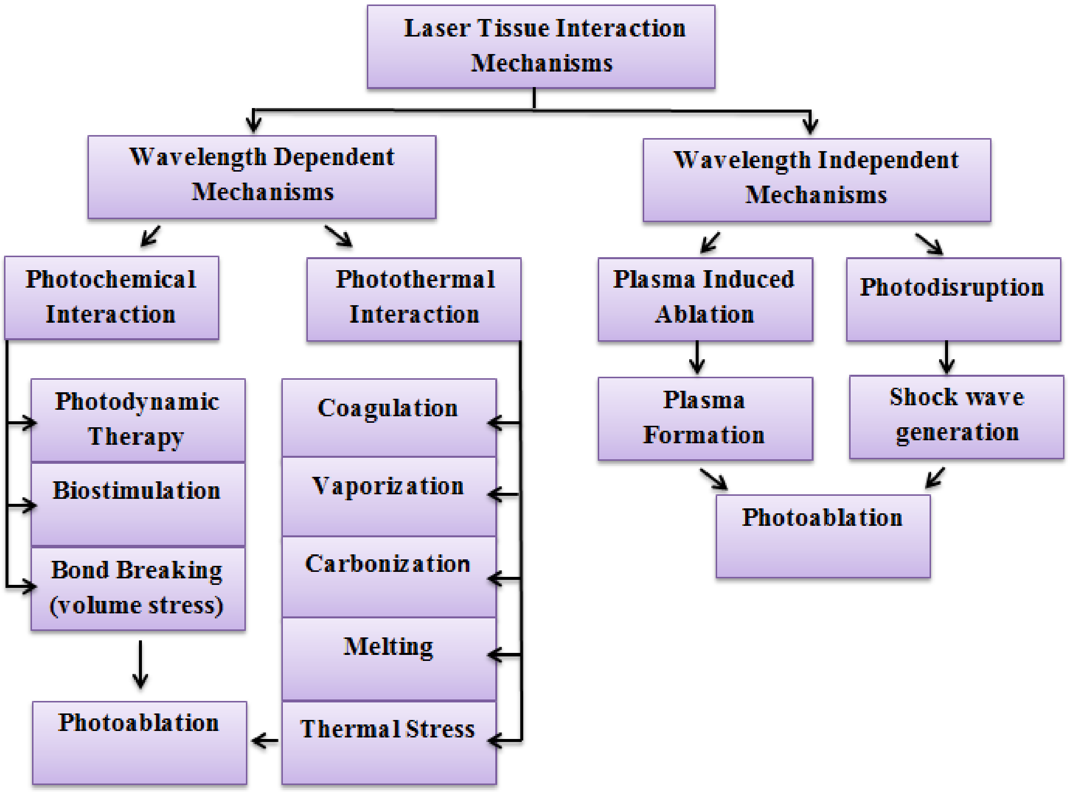

Fig. (1-4): The mechanisms of interactions of laser together with biological tissues [70].

1-6 Laser Safety Criteria and Hazard Classification

Lasers are classified into various categories based on beam's power or energy as well as the wavelength of generated light. The potential for producing flames from exposure directly to the beam or reflections from light reflective surfaces, is used to classify lasers. Labels applied to commercialized lasers are used to classify and identify them. When a laser is made on campus or becomes unlabeled, the laser safety officer (LSO) should indeed be consulted to determine the proper laser categorization and labeling. Lasers are categorized using the physical properties of wavelength, power, and duration of exposure [74]. The classification is built upon the power of beam output or laser’s energy. Essentially, the categorization is meant to define the laser's ability to cause injury to people. The bigger the potential hazard, the larger the categorization number. Basic laser hazards irradiation hazards consistent with the laser class [75] are shown in Table (1-4).

Table (1-4): Basic laser irradiation hazards consistent with the laser class [75].

Class I	Safe, due to very low radiant emission.
Class II	(Covers visible emission only) Possible eye hazard other than for accidental momentary viewing.
Class IIIa	Eye hazard if magnifying viewing instruments are used to view or intercept the beam.
Class IIIb	Hazard to the unaided eye. The viewing of diffuse reflections is normally safe. It Can also exceed the skin safety threshold, but would not be expected to cause serious harm to the skin.
Class IV	Eye and skin hazard. Diffuse reflections may also be hazardous. Possible fire and fume hazard by interaction with target material.

1-7 Laser Applications in Dentistry

Laser uses in dentistry are numerous and depend on the type of laser used. These lasers are diverse from the cold lasers that utilized in phototherapy for pain relief, headaches, and inflammation to elimination of tooth's decay and prepare the enamel surrounding for receiving of the filling. The most important lasers that uses in density are demonstrated in table (1-5).

Table (1-5): Laser uses in dentistry and its characteristics [76].

Laser type	Wavelength Nm	Waveform	Applications
CO_2	10,600	Gated (or interrupted or continuous)	Soft-tissues incision and ablation*;de-epithelialization of gingival during periodontal regenerative procedure
Er:YAG	2940	Pulsed	Caries removal, cavity preparation in enamel and dentin, U.S.FDA** clearance for use on cementum and bone; root canal preparation
Er,Cr:YSGG	2780	Pulsed	Enamel etching, caries removal, cavity preparation, cutting bone in vitro with no burning, melting or alteration of the calcium: phosphorus ratio, root canal preparation
Ho:YAG	2100	Pulsed	Soft-tissue incision and ablation*
Nd:YAG	1064	Pulsed	Soft-tissue incision and ablation*:incipient caries removal
Gallium – Arsenide (or Diodes)	904	Pulsed or continuous	Soft-tissue incision and ablation*
Argon	457 to 502	Pulsed or continuous	Curing resins; soft-tissue incision and ablation*; bleaching

*: including gingival troughing esthetic contouring of gingiva, treatment of oral ulcers, frenectomy, gingivectomy.

** FDA: Food and Drug Administration

1-8 Laser Ablation of enamel and dentin dental hard Tissues

1-8-1 Mechanism of Er,Cr:YSSG Laser Ablation of dental hard Tissues

Many researchers have been attracted to laser ablation of both enamel and dentine during cavity preparation because it is deemed safe, lowers pain, loudness, vibrations as well as discomfort in patients. Due to improvement in its usage in dental tissues, the Erbium:yttrium aluminum-garnet (Er:YAG) (2.94 µm) as well as Erbium, Chromium: yttrium scandium gallium garnet (Er, Cr:YSGG, 2.78 µm) lasers are being extensively explored [77]. The Er:YAG laser had first been characterized in 1989 as having the ability to remove dental hard tissues deprived of generating thermal negative effects on the residual dental tissues, like cracking or charring [54,78]·

Er,Cr:YSGG laser generates photons with wavelength of 2.78 um, that are extensively absorbed by water and hydroxyapatite crystals, which are the main components of tooth structure [79]. When laser energy being concentrated on the tooth, surface layer of tooth, as well as water within it, is rapidly heated. This water vaporizes nearly instantly, and also the steam causes the irradiation volume to grow. The material splits as the expansion exceeds crystal strength of tooth structures. This explosive release of ablated debris begins shortly just after laser irradiation begins and continues till the power is reduced. Because the ablation is done swiftly, only a little quantity of heat is transported to the neighboring tissue. Leftover tissue volumes at crater base and tooth structure illuminated at energy level slightly underneath the threshold of ablation are responsible for heating of a tooth which really does occur. As laser energy is boosted, the ablation threshold gets lowered, which speeds up the ablation time and minimize thermal side effects. Another point to be considered is that as whenever the energy level rises, so does the velocity profile of the ejected material, resulting in more profound effect on the intended location. The increased effect causes more mechanical withdrawal symptoms, with higher irradiation, plasma is also generated, reducing efficiency significantly. Covering the operating area with a fine film of water is indeed a convincing way to reduce heat without adding energy [80].

The resulting high stream pressure leads to the occurrence of successive microexplosions with ejection of tissue particles [70,81].

The microexplosions are characteristics of the ablation process and determine the microcrater like appearance of the lased surfaces [78] .

So that, the ablation of tooth structure is achieved via a themomechanical ablaion, with the majority of incident radiation is consumed in the ablation process, leaving very little residual energy for adverse thermal effects on the pulp and the surrounding soft and/or hard tissues [82].

Fast subsurface expansion including its interstitially stuck water inside mineral substrate generates a tremendous volume expansion, which causes adjacent material to be ablated away. A small amount of heat energy is delivered to the remaining neighboring tooth structure due to water spray as well as short pulse length [83]. When laser interacts with dental tissues, popping sound produced with all erbium lasers. The photoacoustic impact is the name given to this popping noise. The pitch and the resonance of such a sound wave depends greatly on whether the tooth is decayed or not [84,85]. This photoacoustic outcome is feature of pulse duration that is short (100–250 μs) as well as high energy density [86]. In complement to a photoacoustic impact, erbium lasers have bactericidal impact, identical to other wavelengths [87-89]. Water within bacterial cells absorbs the erbium wavelength, as well as the cells encounter the same liquid-into-steam evaporation seen throughout hard tissue ablation [90]. One of extra benefits for employing lasers throughout soft and hard dental tissues treatment is eradication of microorganisms. Hard tissue lasers biophysics have always been and continues to be a contentious topic.

1-8-2 Mechanism of Nd:YAG Laser Elimination of dental hard Tissues

Nd:YAG laser stands for Neodymium: yttrium-aluminum-garnet, which is a yttrium-aluminum-garnet crystal (YAC) that has been doped with neodymium. The laser operates in the infrared band (1.06 μm) thus, similar to CO_2 lasers, is invisible [91]. The Nd:YAG laser has the benefit of being able to be transported through a fiber and supplied as a result using fiber optic technology. They have unrestricted access to the mouth [73].

The Nd:YAG laser is being appealing to pigmented tissue, owns varying degrees of light scattering in addition to tissue penetration, low degree of absorption, nevertheless no reflection. This laser may be utilized in both contact as well as non-contact mode, and that's a great tool for tissue coagulation, ablation, and incision. The Nd:YAG laser with a wavelength of 1064 nm may penetrate water to a distance of 6 cm before attenuating to 10% of its initial intensity. As a result, instead of being absorbed on tissue surface and so is the case with CO_2 laser radiation, the energy is dispersed in soft tissue. However, because this wavelength is drawn to colors, dispersion is roughly twice as high as absorption in densely colored soft tissue like skin. The Nd:YAG laser's heating impact is appropriate for ablation of possibly hemorrhagic aberrant tissue, as well as hemostasis of tiny capillaries and venous vessels [92].

However, because the surface color of, tissue is not a dependable sign of heat injury, the scattering effect makes assessing the depth of diffusion more difficult, especially into pale colored tissue. Whenever the device was utilized to eliminate the smear layer off dental roots in vitro, there was a considerable increase in intra pulpal heat injury [93,94]. The contact tip provides tactile feedback for the surgeon, which is not accessible with non-contact Nd:YAG or carbon dioxide lasers or Er:YAG lasers. However, the degree of tissue damage was still higher than with a standard scalpel [95]. Using specially built hand pieces having contact and non-touch probes, the Nd:YAG laser system, intended and advertised for oral a well as dental applications, which can provide up to 3 w of power. In 1990, the FDA approved it all for oral tissue. The FDA, on the other hand, has prohibited any laser producer from claiming that it can disinfect an area or that it is harmless [96].

Water does have an absorbance peak in the Nd:YAG lasers wavelength range, but the major or biggest absorbance peak is in the 3 μm range, which is why Er:YAG is used. Water absorbs the YAG laser efficiently [70]. The coefficients of absorption (α) and the depth of penetration (L) of Nd:YAG laser is 0.61 cm^{-1} and 1.6 cm accordingly into water, whereas for Er:YAG laser α is about 12000 cm^{-1} and L matches to 0.00008 cm into water [70], whereas in the tissue the depth of penetration for Nd:YAG laser span 2-5 millimeter in the tissue [76].

Because the Nd:YAG laser absorbs effectively in pigmented tissue, a decayed lesion could be considered a pigmented tissue, and thus the Nd:YAG laser could be utilized to treat incipient caries. Some have suggested that photo absorbing black dyes be applied topically to the tissue to improve energy uptake on the surface [76,97]. Meanwhile, due to heat condensing and subsequent evaporation of organic components of tissue, which results in tissue carbonization, vaporization throughout healthy tooth structures cavity preparation using Nd:YAG laser would take much longer. These carbonized layers will boost Nd:YAG laser absorption [76].

1-9 Methods Used in Determining Temperature Changes

A sum of methods has utilized when quantifying changes in temperature in vitro including:

1. Infrared thermography [98] by means of infrared apparatus quantifying temperature beginning from 0-500 ^{0}C that has three channels in order to record ambient temperature, humidity of room, and measured temperature of the surface.

2. Thermocouple measurements using tooth sections [78,99] as well as a thermocouple measurement among whole teeth that could be placed on the outside surface of the tooth or else placed into the pulp chamber by utilizing thermocouple probe which attached with thermometer [63].

3. Thermistor is a resistance thermometer, or a resistor whose resistance is dependent on temperature. The term is a combination of “thermal” and “resistor”. It is made of metallic oxides, pressed into a bead, disk, or cylindrical shape and then encapsulated with an impermeable material such as epoxy or glass.

The previous surveys show that the measured of the temperature rise have been employed throughout composite resin polymerization utilizing a thermistor [100,101], thermocouples [29,102-106] as well as infrared thermography [55,107]. These investigations, on the other hand, exclusively assessed temperature changes at the lower surface of composites [100,102], [101], at the pulpal wall of dentin [29,104,105] or at the middle region of composites[103,106]. Lately, Chang et al. [108] was used the infrared thermography, which the researchers assessed the polymerization temperature across multiple locations anywhere along external surface of such Class II cavity based on the curing depth as well as proximity to the cavity wall . A thermal image could now be captured using a thermos camera, which can then be registered and analyzed using scientific imaging software [109].

Now a days, all optical fiber founded temperature sensor applications have progressed amazingly and is now begun to truly challenge other traditional temperature sensors, since it is founded on bulk structures or materials [13]. Furthermore, they are good enough for accomplishing distributed as well as multi-point analysis, which allow for the monitoring the temperature in different points of ambiguous tissue via insertion of condensed sized, facile structured sensor appliance. [2,19]. In addition to the mentioned appreciated properties, optical fiber sensors have also good accuracy (finer than 1^0C), high sensitivity, cost efficacy, conciseness, soundness, possibility of distant sensing, high-rise sensitivity, as well as vulnerability to electromagnetic interference. Furthermore, they are chemically plus biologically passive and could be joint with complex setups for real time multi parametric sensing [110,111].

1-10 Optical fiber sensors (OFSs):

Fiber optic cable is indeed a dielectric waveguide that is flexible and transparent and has various protective coatings. It is made up of 2 cylindrical rods, usually composed of plastic or glass, that have differing doping levels. A transparent core (with a diameter of almost 5-100 μm) is wrapped by a cladding with a somewhat reduced refractive index (almost all of the cladding does indeed have a diameter of approximately 125-200 μm) within those fibers. An extra plastic coating of buffer layer is applied to the cladding providing environmental protection as well as mechanical support [112]. A typical cross section of conventional single mode fiber is shown in figure (1-5). Optical fiber has indeed been widely used as a waveguide because of its resistance to electromagnetic field influence and minimal signal loss. When light is transmitted via the two ends of the fiber, it propagates contained within the core due to the phenomena of "total internal reflection". Total internal reflection happens when the incidence angle is larger than the critical angle, as according Snell's law [113], as revealed in figure. (1-6).

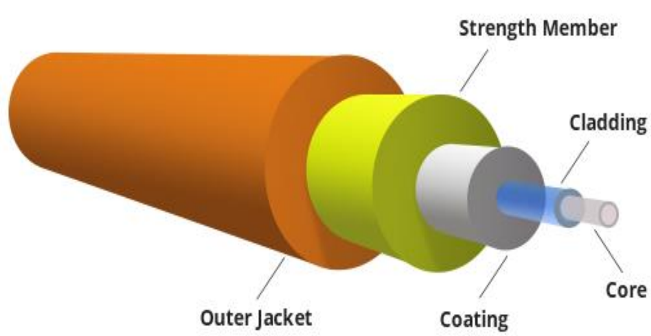

Fig. (1-5): conventional structure of optical fiber [113].

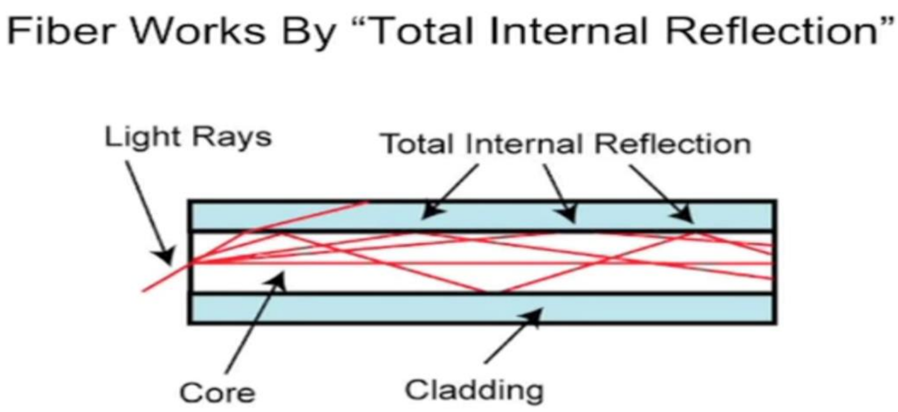

Fig. (1-6): total internal reflection inside an optical fiber [113].

Optical fiber sensors (OFSs) witnessed rapid development in the fields of optoelectronics as well as the optical fiber communication [114]. Optical fibers have been used as recognizing devices in a variety of sensing applications, including medical sciences [115], natural configurations [116], biological group [117], analytical chemistry [118], environmental condition [119], as well as additional physical parameters [120]. Because OFSs offer various magical benefits over electronic sensors let's say it can merely be incorporated inside structures because of to their comparatively small size as well as cylindrical geometry, creating what is recognized as smart configurations. These are in addition purely dielectric; consequently, they are appropriate to be utilized simply in hazardous zones, as well as are resistant to electromagnetic interference. Furthermore, they are tough, lightweight, plus have broader bandwidths in addition to these advantages; enrichments in the sensitivity along with cost reduction have been also momentous interest in OFS during the latest decade [121].

Generally, at curves in their courses, optical fibers experience radiation losses. This really is owing to the evanescent field's energy surpassing the cladding's light velocity at the curve. Bends are divided into two types: Macro bend loss which refers to losses generated in bends around mandrels of a specified diameter. Microscopic bends with radius of curvature approximating to the fiber radius mustn't be produced in the fiber cabling process. These so-called micro bends loss denotes to specified minimum scale "bends" in the fiber, often from pressure applied on the fiber itself. But on the other side, Mach–Zehnder interferometric structures founded on macro bent optical fiber (e.g. balloon-like shape, U-shape, S-shape, etc.) have been extensively studied for constructing miniature RH sensors owing to their cost efficacy, system easiness, no need for preprocessing, suitable accuracy, as well as greater constancy, which severely releases their usefulness in definite sensor systems, as well as their capacity to sweep large field with excellent measurement repeatability [122-125]. In the present work, the balloon-like fiber construction comprises a division of SMF and also a capillary tube to boost twisting SMF hooked in balloon-like configuration, which is modal interferometer founded on MZI principle could be created with a proper bending radius. As light signal travels through the bent part, the MZI begins to work, allowing portion of the light to escape the core border and enter the cladding. At the bend's waist, light would couple back through fiber core. The modal interference is formed by the variation in optical pathway length between both the cladding as well as core modes [113,126]. Essentially, the usual one achieves this deformation by bending the fiber into a series of circle or semi-circle shapes with small bending radii. So, many bend path leads to repeat this process and then more improvement in the sensor sensitivity [127,128]. Additionally, this basic idea behind these sensors relies on that, as the fiber is bent over a critical diameter, the optical energy of the guided mode suffers loss as long it travels along the bent section because of the sudden variation in the critical angle [129]. Bending loss in optical fiber is determined by the fiber's characteristics, the surrounding medium in contiguity with the bent region, and the bending curvature diameter, which have to be precisely modeled for sensing application [130].

Furthermore, the dimensions are particularly delicate to the measuring of numerous physical characteristics such as temperature, additional to the refractive index of both fiber core as well as cladding. Thermal expansion coefficient, photo-elastic characteristics of silica fiber, fiber core refractive indices, and diameter of the core, intrinsic thermo-optic impact coefficients, and fiber length all seem to be heat dependent. Henceforth, the spectral shift for the transmitted spectrum within the fiber alters together with the surrounding temperature [131].

1-11 Literature survey:

Throughout laser ablation, heat generation must be considered. Painful sensations are possible, especially when laser ablation is performed near pulpal tissues. As dentine pulp complex can be irreversibly damaged by heat. It is necessary to investigate the role of residual dental tissue thickness in the heat changes observed in pulp tissue.

In 2010, Laura Emma *et .al.* [132] after irradiation using Er:YAG laser having energy of 100 mJ, fluence of 12.7 J/cm^2, and along with 150 mJ energy, fluence of 11 J/cm^2, at 10 Hz with water spray, the structural and morphological alterations of the enamel were investigated. The AFM images showed cracks with depths between 250 nm and 750 nm for Groups II and IV, respectively, and the widths of these cracks were 5.37 mm and 2.58 mm. The interior of the cracks showed a rough surface. The SEM micrographs revealed morphological changes. Significant differences were detected in Ca, P, and Cl in the crater and its periphery.

In 2011, Al Qaradaghi *et al.* [133] found that reducing remaining dentin thickness resulting in a greater intra-pulpal temperature rise. Results showed that laser ablation caused less temperature rise than conventional bur during cavity preparation taking into account the invitro temperature rise of class V cavity preparation. The maximum temperature variation for Er;YAG laser and conventional bur were 2 °C and 3 °C respectively in 1mm depth, and 2 °C and 4 °C respectively in 2mm, temperature elevation less than 5 degree C considered non threaten to pulp tissue. (Zach and Cohen,1965) nevertheless Er:YAG laser showed a better results than conventional bur.

In 2012, Janez Diaci *and* Boris Gaspirc [134] stated that erbium lasers provide the safest as well as most efficient solutions among the available Erbium laser equipment, Er:YAG and Er,Cr:YSGG, offers maximum absorption characteristics, along with cold ablation achievable when using minimally invasive small pulse energies. When used on hard dental tissues, the Erbium laser energy heats up the water within the hard tissue and causes that water to be turned into steam. This causes a mini-explosion to occur and the hard tissue is "ablated" (removed). Ideally, the remaining dental tissue beneath should not be affected by the Erbium laser ablation, thereby allowing precise control and minimal damage to the surrounding tissue. The Erbium lasers attained their original target to supplement as well as improve the confines of the traditional mechanical devices in the dentist's office.

In 2013, Marina *et al.* [135] The infrared pyrometer used (RAYMIC20LTCB3V, Raytek Co., Santa Cruz, CA, USA) allowed non-contact infrared temperature measurements between −40 and 600 °C. Its sensing head was coupled to an aluminum structure, in which an aperture of 4 mm diameter was drilled. The sample was positioned on this aperture, and its upper surface irradiated. Concomitantly, the temperature radiation emitted from the opposite surface was directed to the sensing head by an aluminum mirror. The temperature profile over time was recorded by a computer and the device software (Marathon MI Series 4.7.5, Raytek Co.). Using this sensor, identification of the feasibility of using ultra-short pulsed lasers (USPL) in restorative dentistry while keeping the well-known effects of lasers for caries eradication and also avoiding drawbacks for instance thermal insult of the treated substrate was done.

In 2014, Cantekin *et. al.* [136] compared temperature rises in the pulp chamber induced by halogen, plasma arc, and conventional light-emitting diode (LED) curing units with that induced via a new generation LED-curing unit (VALO) in extra power mode. a thermocouple wire (AB 25 NN, Thermocoax, Heidelberg, Germany) was inserted into the pulp chamber of each tooth to measure temperature changes. The wire maintained immediate contact with the dentin via a thin layer of silicon oil-based thermal joint compound. The greatest temperature increases were observed during polymerization of composite resin with a halogen curing unit (3.2 degrees Celsius), followed by plasma arc curing (2.07 degrees Celsius) and VALO curing (1.44 degrees Celsius); the lowest temperature rise was with conventional LED curing (1.01 degrees Celsius).

In 2015, Runnacles *et.al*. [137] evaluated pulp temperature rise in human premolars during exposure to a light curing unit using selected exposure modes. A wireless, NIST-traceable, temperature acquisition system (Temperature Data Acquisition – Thermes WFI, Physitemp Instruments Inc., Clifton, NJ, USA) was used. All emission modes produced higher peak pulp temperature than the baseline temperature ($p < 0.001$).

In 2016, Andreatta [138] evaluated the temperature variation inside the pulp chamber during light-activation of the adhesive and resin composite layers with different light sources. The variation of pulp chamber temperature was measured with a K-type thermocouple sensor connected to a CPM-45 thermometer (Contemp, São Caetano do Sul, SP, Brazil). The thermocouple was inserted into the pulp chamber and placed in the center of the cavity in contact with the inner axial dentin wall. Higher temperature increases were observed with the adhesive and the first resin composite increment light-activation, regardless of the employed light source.

In 2017, Cleide *et. al*. [139] evaluated intra-chamber temperature increase on 12 standardized teeth extracted human teeth exposed to 670 nm wavelength laser diode. Type-K thermocouple wire with a 0.5 mm diameter probe was inserted into the tooth pulp chamber (ICEL-Manaus-brand). The laser device (lasotronic-brand InGaAlP) laser diode was used to irradiate tooth enamel, perpendicularly to the external surface for 30 secs, with power of levels of 340, 272, 204, 136, and 68 mW. The measurements were taken at three time points: 0, 30 secs, and 3 min after the laser irradiation. The highest ΔT (ΔT = final temperature–initial temperature) values obtained were observed to incisors with 340 mW, 272 mW; 204 mW of power (respectively 4.7°C, 4.2°C, and 3.1°C); and canines presented the lowest ΔT (0.8°C–0.3°C) with no influence of power output**.**

In 2018, Fan *et. al.* [140] compared pulp chamber temperature changes of Nd:YAP laser, Nd:YAG laser and semiconductor laser with the same power during dentin hypersensitivity treatment, and evaluated the safety of these three laser treatments for dentin hypersensitivity. Thermocouple thermometer was used to record the temperature changes in the pulp chamber. The smallest temperature rises was in the Nd:YAP laser group, followed by the semiconductor laser group, and the temperature rise was highest in the Nd:YAG laser group, but it was still lower than 5.5 ° C that could cause pulp necrosis.

In 2019, Ra'fat [141] studied the effect of cooling water temperature on the temperature changes in the pulp chamber and at the handpiece head during high-speed tooth preparation using an electric handpiece. The temperature changes in the pulp chamber and at the handpiece head were recorded using K-type thermocouples connected to a digital thermometer. The average temperature changes within the pulp chamber and at the handpiece head during preparation increased substantially when no cooling water was applied (6.8°C and 11.0°C, respectively), but decreased significantly when cooling water was added. The most substantial drop in temperature occurred with 10°C water (−16.3°C and −10.2ºC), but reductions were also seen at

23°C (−8.6°C and −4.9°C). With 35°C cooling water, temperatures increased slightly, but still remained lower than the no cooling water group (1.6°C and 6.7ºC).

In 2020, Kamath *et. al.* [142] had used a laser-guided IR thermometry like an auxiliary method for assessing pulp vitality between vital as well as non-vital teeth. There were no significant changes in baseline temperature. Vital teeth however have better surface rewarming as compared to non-vital or diseased teeth. Laser guided IR thermometry on the other hand, have excellent surface rewarming than non-vital and diseased teeth. It is a simple and reliable technology which can be used like a routine pulp vitality check in a clinical setting. Infrared Thermography's non-harmful nature may also contribute to enhanced collaboration and patient compliance throughout diagnostic procedures.

In 2021, Kaushik *et al.* [143] evaluated and compared the changes in pulp chamber temperature during direct fabrication of provisional restorations in maxillary central incisors after using three different cooling techniques using K-type thermocouple wire that inserted in the tooth and secured at the pulpal roof using amalgam. Teeth were sectioned 2 mm below cementoenamel junction and a. Putty index filled with DPI tooth molding resin material [polymethyl methacrylate (PMMA)] was placed on the tooth and temperature changes per 5 seconds were recorded by temperature indicating device for the control, on–off, precooled putty, and dentin bonding agent (DBA) group. The highest mean obtained was of the control (11.04°C), followed by DBA group (9.53°C), precooled putty group (6.67°C), and on–off group (1.94°C). Precooled putty index group took maximum time to reach the baseline temperature (847.5 seconds).

1-12 Aims of the study:

1. To establish the efficiency of a novel technique of temperature measurement using optical fiber sensor that possesses ultrashort response time

2. For instant measurement of temperature rises in dental tissues after laser radiation.

3. To examine the impact of Nd:YAG laser with wavelength of 1064 nanometer and Er,Cr:YSGG of 2780 nanometer wavelength on pulpal vitality, during cavity preparation on the buccal surface of samples.

4. Establish the standards for dentists and laser manufacturers (healthcare professionals) that should be followed to decrease the probability of pulpal necrosis while handling the tooth structure for cavity preparation purposes.

Chapter Two

Materials and Methods

Chapter Two

Experimental Methodology

2-1 Materials and Methods

All information of our work, materials, methods, and preparations will be described comprehensively in the following sub-sections. But firstly, the most important specimens and devices that are used in the present work are listed as follows:

1. A total of 110 healthy, caries-free human maxillary and mandibular premolar teeth were extracted for orthodontic purposes.
2. Nd: YAG laser (Quantel Brilliant b), France.
3. Er,Cr:YSGG laser (Waterlase iplus, BIOLASE Technology, USA).
4. Er,Cr:YSGG laser handpiece with fiber containing 600 μm in diameter (tip model: ZipTip MZ6 6mm) .
5. Physiological saline solution, Iraq.
6. Double-sided mini diamond disk with a flexible 0.15 millimeter thickness (handpiece tip), Brazilian.
7. Fissure bur made of carbide (straight fissure, 8-fluted and 0.9 millimeter diameter), China.
8. Clamp.
9. Convex lens of 5 cm focal length, Iraq.
10. 3-D linear- computer-controlled micrometer translation stage. Custom made, Iraq.
11. Hot plate of changeable temperature, China.
12. Vacuum chamber. Custom made, Iraq.
13. Heat conductive paste (carbon paper), Iraq.
14. Metal gauge. China.

15. Yokogawa AQ6370 optical spectrum analyzer (OSA) with 0.02 nm resolution, Japan.
16. Broadband light source (Thorlabs SLD1550S-A1) with a wavelength range of 1450–1650 nm, USA.
17. Rubber cup, Switzerland (Products Dentaires S.A.).
18. Sub gingival ultrasonic scaler, WOODPECKER HW-5L, China.
19. Rail.
20. High-speed handpiece (conventional drill) (NSK PANA-MAX) with water spray, Japan.
21. Low-speed handpiece with water spray (NSK EX-203C), Japan.
22. Single mode fiber, coring (SMF-28). USA.
23. Capillary tube. Jordan.

In this experiment, fiber optic grounded on the balloon-like construction was used as temperature sensor.

Fig. (2-1): Materials used to prepare specimens (A) double sided mini diamond disk. (B) High speed handpiece, (C) subgingival scaler, (D) Rubber cup, pumice and low speed handpiece, (E) metal gauge, and (F) Physiological saline solution with teeth samples.

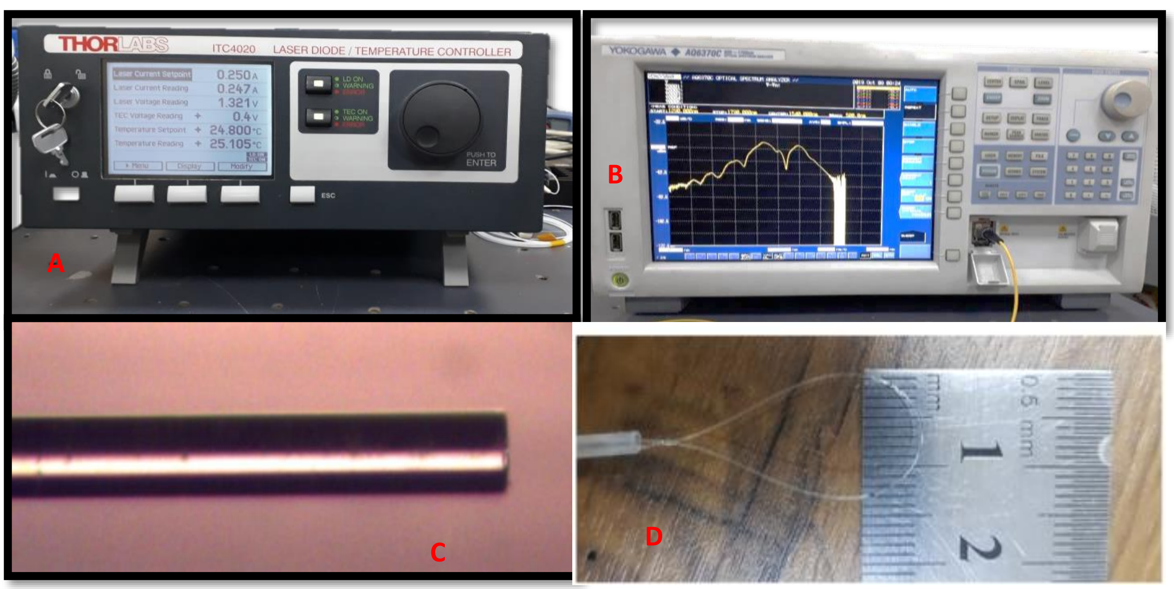

Fig. (2-2): devices used to measure the temperature rise: (A) broadband source, (B) optical spectrum analyzer (OSA), (C) Top view for the SMF under an optical microscope with magnification power (4x) magnification, and (D) balloon-like shape fiber sensor.

2-1-1 Sample Collection

In this work, non-carious maxillary and mandibular 1st and 2nd premolar teeth extracted for orthodontic reasons were collected and preserved in saline solution at room temperature. Then, for removing any calculus deposits, these specimens were scaled using ultrasonic scaler, then polished with pumice and rubber cup

In the first step, the collected teeth were checked using a magnifying lens to rule out any teeth having surface cracking out of the study.

2-1-2 Samples Grouping

The collected 110 teeth samples were grouped into two major groups, which each group consists of 55 of teeth samples:

- The 1st group represents samples irradiated with Nd:YAG laser.
- The 2nd group represents samples irradiated with Er,Cr:YSGG laser.

Then, each of the above groups was subdivided into subgroups, which each subgroup consists of 11 teeth that subdivided as:

- Group 1: Consists of temperature changes in 1 mm thickness of enamel hard tissue.
- Group 2: Consists of temperature changes in 2 mm thickness of enamel hard tissue.
- Group 3: Consists of temperature changes in 1 mm thickness of dentin hard tissue.
- Group 4: Consists of temperature changes in 2 mm thickness of dentin hard tissue.
- Group 5: Consists of temperature changes in 3 mm thickness of dentin hard tissue.

2-1-3 Sample Preparation

Freshly extracted caries-free upper and lower premolars, extracted for orthodontic purposes, were collected. The teeth were extracted for orthodontic purposes from various patients with age range (10-٣٥ years) and preserved at room temperature in a physiological saline solution. The patients had informed that extracted premolars would be used in an in-vitro experiment. Scaling and polishing of teeth was done to remove any calculus deposits and stains that were present. Teeth were segmented longitudinally to their long axis, using a flexible 0.15 mm thickness double-sided mini diamond disk (handpiece tip), and pieces of about 4 mm thickness were got. Then these pieces were reduced using low-speed dental handpiece carbide fissure bur (straight fissure carbide bur, 8-fluted, 0.9 mm diameter), utilizing a grinding system (low-speed handpiece, rpm 20,000, EX203C) by water spray, till a thickness of 1, 2 and 3 mm was attained. Samples were preserved in purified physiological water saline throughout the experiment. Using Nd:YAG laser, standardized cavities (4×3 mm mesiodistally) were prepared on the buccal surfaces of half of the specimens. For Nd:YAG laser, teeth were painted (blue areas) with heat-conductive paste (carbon paper) to facilitate the absorption of laser energy (white areas) throughout laser irradiation as shown in figure (2-3). Then by using Er,Cr:YSGG standardized cavities were prepared on the buccal surfaces of the other half of the specimens. See figure (2-4).

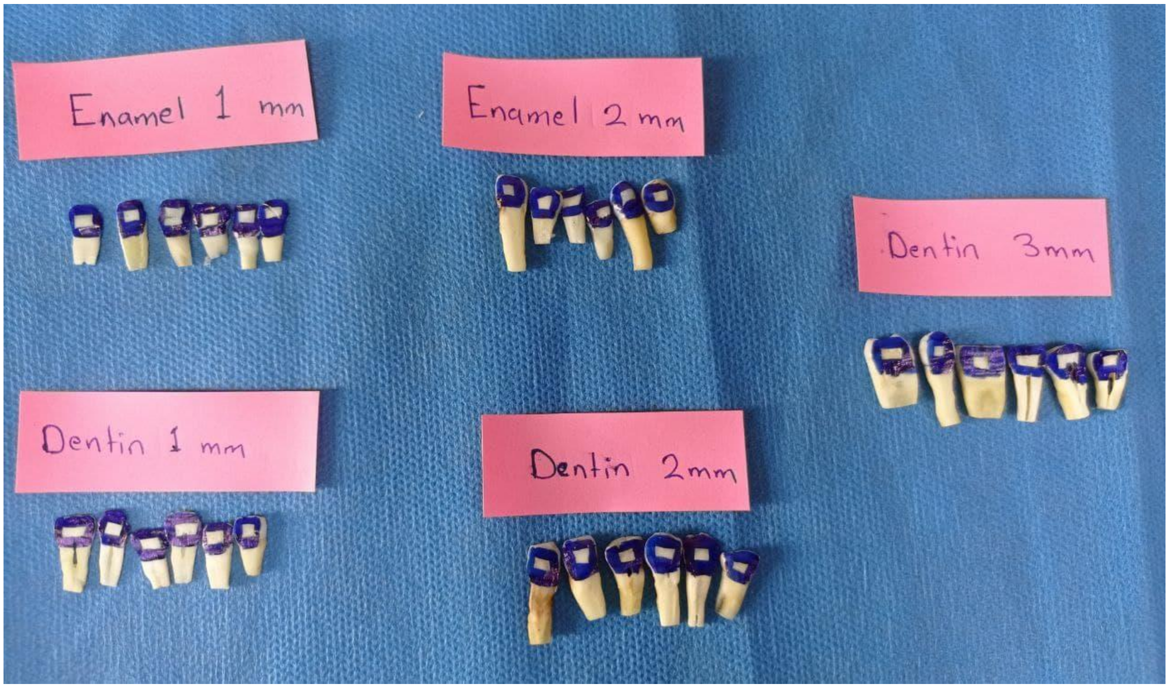

Fig (2-3): samples irradiated with Nd:YAG laser.

Fig (2-4): samples irradiated with Er,Cr:YSGG laser.

2-1-4 Laser Device

In this experiment, teeth samples had irradiated by two lasers. The first laser is infrared Q-switched Nd:YAG laser of pulse duration 9 ns, a 10 Hz repetition rate, and a total energy of 850 mJ and an average power of ~8.5 W. These samples irradiated with Nd:YAG laser using heat conductive paste without any cooling or water spray. The laser head is placed at 10 cm from the dental hard surfaces, a 5 cm focal length lens was used to concentrate the laser beam on the sample. The spot size of the laser pulse is 1 mm fixed at constant distance which is important to confirm a steady beam diameter for each ablated sample.

The second laser is Er,Cr:YSGG (Waterlase iplus, BIOLASE Technology, USA) with 2.78 um wavelength, pulse duration of 60 μs, energy of 260 mJ, repetition rate of 15 HZ and power of 4 W have been inspected but in the situation of damp ablation. Cooling off all through the cavity preparation has been done with rate of water spray 50% and 80% air. In a non-contact mode, laser irradiation was conducted perpendicular to the specimen' buccal surface at a distance of 2 mm from the laser tip. Each tooth was irradiated for total of 15 s. The experimental setup is shown in figure (2-5).

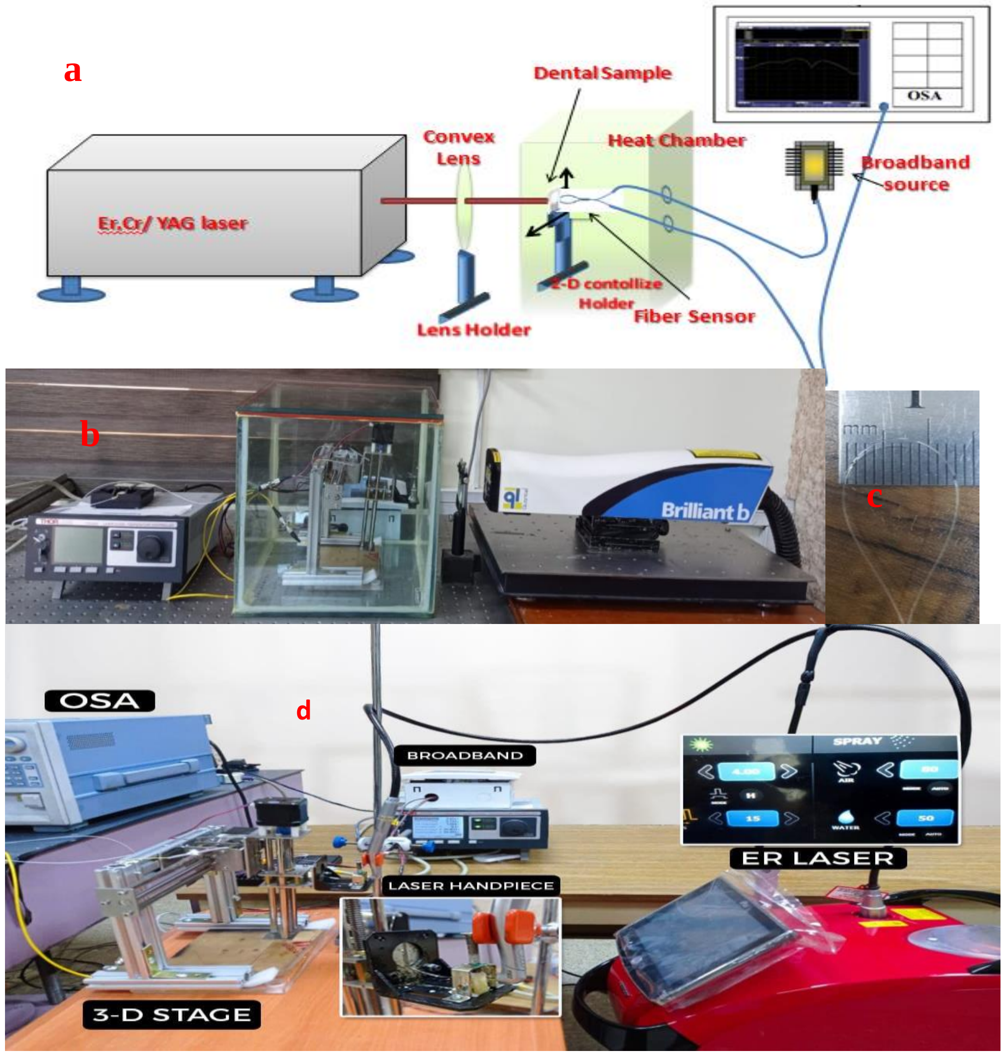

Fig. (2-5): (a) schematic diagram, (b) the experimental setup of the Nd:YAG laser, (c) fiber sensor, (d) the experimental setup of Er, Cr: YSGG laser.

2-1-5 Sample Mounting and Cavity Preparation.

For Nd:YAG laser, the samples are fixed on a 3-D linear, computer-controlled micrometer translation stage to shift it along the ray axis of the focused pulsed laser. As utilizing this scanner system, rectangular cavities with a 4 mm length are made in the non-contact mode. The schematic diagram of the present experimental setup is shown in figure (2-5 a,b,c).

While, for Er,Cr:YSGG laser irradiation was performed perpendicular to the buccal surface in non-contact mode with fixed at distance of 2 mm away from the laser tip. The laser handpiece was fixed by clamp to ensure consistent distance and subsequently constant energy density and spot size. The entire period of irradiation for each sample was 15 sec. Diagram of the present experimental setup is shown in figure (2-5 a, c, d.).

2-1-6 Fiber Sensor and Temperature Measurement

During cavity preparation, temperature measurements are performed using a temperature fiber sensor attached to the back of the samples. The fiber thermometric balloon-like shape construction setup is shown in figure (2-6). This system consists of a broadband source of light having a wavelength range between 1450 and 1650 nm that is combined with sensor head at the lead-in to deliver light into the balloon-like shape construction, whereas the lead-out of the fiber sensor is united to an optical spectrum analyzer (OSA, Yokogawa AQ6370) having a 0.02 nm resolution for examination of the temperature variation.

Firstly, to verify the sensitivity/responsivity of the fabricated fiber thermometric balloon-like shape construction for temperature, the sensor head was positioned in contact with the hot plate surface with changeable temperature. The examination had performed through raising the temperature starting from 21 ^{0}C to 33 ^{0}C in stages of 2 ^{0}C utilizing the temperature-measured cavity. The spectral examination, the linear fitting of resonant dip shifts versus the temperature variation as well as the time response are examined as shown in figure (2-7).

From these results, it can be found that the fabricated thermometric fiber sensor exhibited a great sensitivity of about 1.975 nm/^{0}C, a high linear regression coefficient (R^2) of 0.993, and a fast response time. Additionally, there is about a 2 nm shift in the resonant wavelength for each rising 1 ^{0}C. This sensor possesses a rise time of 1.45 ms, a recovery time of 2.73 ms, and a fast response time of about 1 ms. For more details about the operation principle of the proposed sensor, see ref. [20,123,128].

Therefore, the laser heating temperature of the dental hard tissue was analyzed using the thermometric fiber sensor above. Using translation step, the tip of fiber sensor was aligned to the laser beam's optical path for all measurements. To determine the base line value, temperature measurements began 1 s before the ablation process began. At intervals of 1 s, additional temperature measuring values were calculated until the maximum temperature reading reached. All measurements were performed in a room where a constant temperature of 21 °C was observed by an air conditioning system.

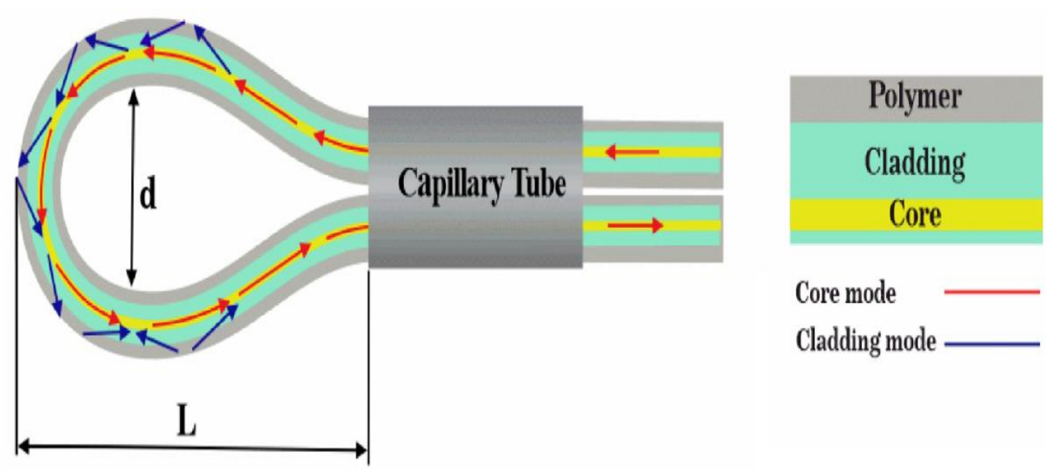

Fig. (2-6): The schematic diagram of the fabricated fiber thermometric balloon-like shape construction.

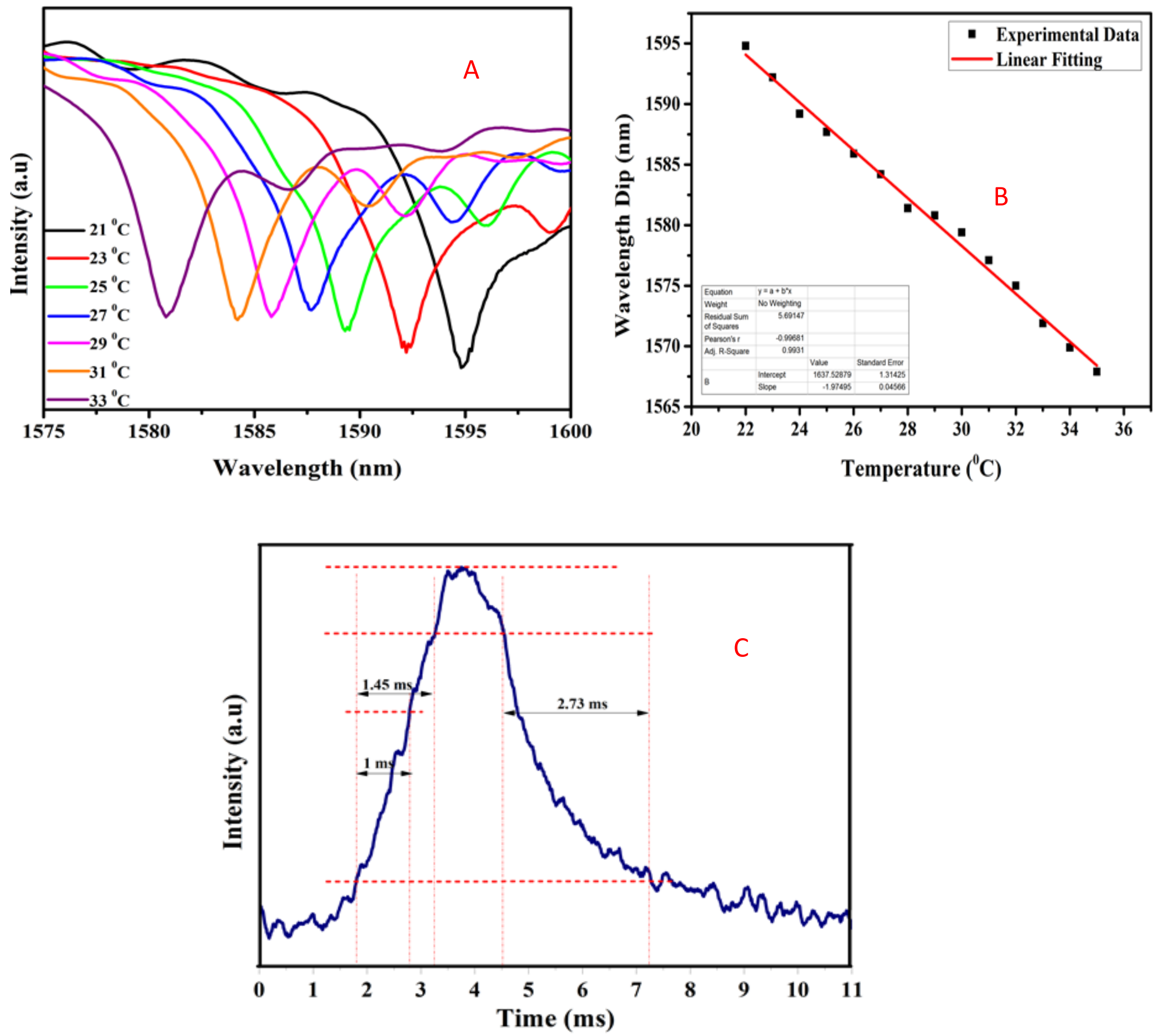

Fig. (2-7): (A) Spectral response, (B) Resonant dip changes' linear fitting versus the temperature variation, and (C) Temporal response of the fabricated thermometric fiber sensor.

2-2 Statistical Analysis

Data were investigated using one-way analysis of variance (ANOVA) test. Analyses were conducted at a significance level of a = 0.05. For statistical analysis, SPSS package Statistics (v 23/ France) was used. The statistical analysis consists of:

1- Descriptive Statistics:

- Means
- Standard deviations (SD).
- Minimum value.
- Maximum value.
- Standard errors (SE).
- 95% Confidence Interval.
- Variances.

2- Inferential Statistics:

- Analysis of variance (ANOVA) test to determine if there is a significant difference among the means of subgroups and groups.
- significance P value was referred to difference among subgroups and groups.
- Paired t-test is used to compare between each pair of subgroups and group for each treatment.
- Tukey post hoc test.

P > 0.05 **NS** (**N**ot **S**ignificant)

P ≤ 0.05 **S** (**S**ignificant)

P < 0.01 **HS** (**H**ighly **S**ignificant)

Chapter Three

Results, Discussion, conclusion and Future Work

Chapter Three

Results, Discussion, conclusion and Future Work

This chapter incorporates the results of the study work, discussion of the end results, conclusions as well as the future work will be stated.

3-1 Results

The results in this chapter include temperature increases examination, statistical analysis, surface morphology of enamel and dentin samples using AFM (atomic force microscopy) and chemical composition of irradiated samples using FTIR (Fourier transform infrared spectroscopy test).

3-1-1 Temperature Increases Examination

In this section, the temperature rises in both enamel as well as dentin samples has been examined using Nd:YAG Laser and Er,Cr:YSGG Laser, respectively.

3-1-1-1 Temperature Increases Examination for Samples Irradiated with Nd:YAG Laser

Heat production have been noticed during the ablation of enamel and dentin samples. Generally, enamel samples exhibited a greater rise in temperature than the dentine samples. Nevertheless, the thickness of the corresponding specimen will determine temperature rise. The lowest temperature could be detected in the 3 mm thickness group of dentine (mean temperature 2.35 ^{0}C) and in the 2 mm thickness group of dentin (mean temperature value 3.22 ^{0}C). The highest temperature increase detected in the 1 mm thickness group of both enamel (mean temperature value 5.59 ^{0}C) and dentine (mean temperature value 5.45 ^{0}C). The results are depicated in figure (3-1).

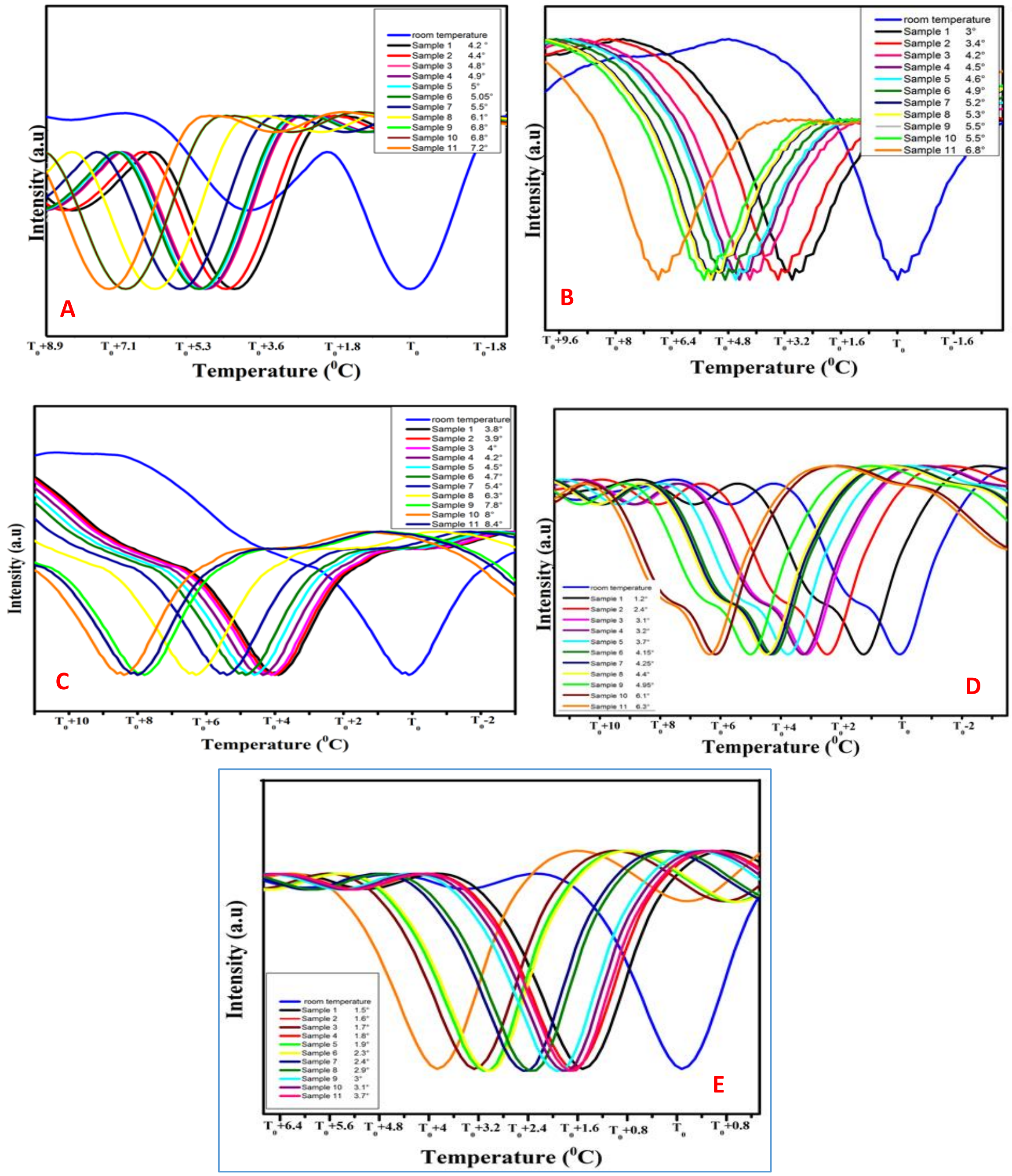

Fig. (3-1): Temperature increases examination after laser irradiation with Nd:YAG laser, (A) Enamel 1mm, and (B) Enamel 2mm, (C) Dentin 1 mm, and (D) Dentin 2 mm, and (E) Dentin 3 mm.

3-1-1-2 Temperature Increases Examination for Samples Irradiated with Er,Cr:YSGG Laser

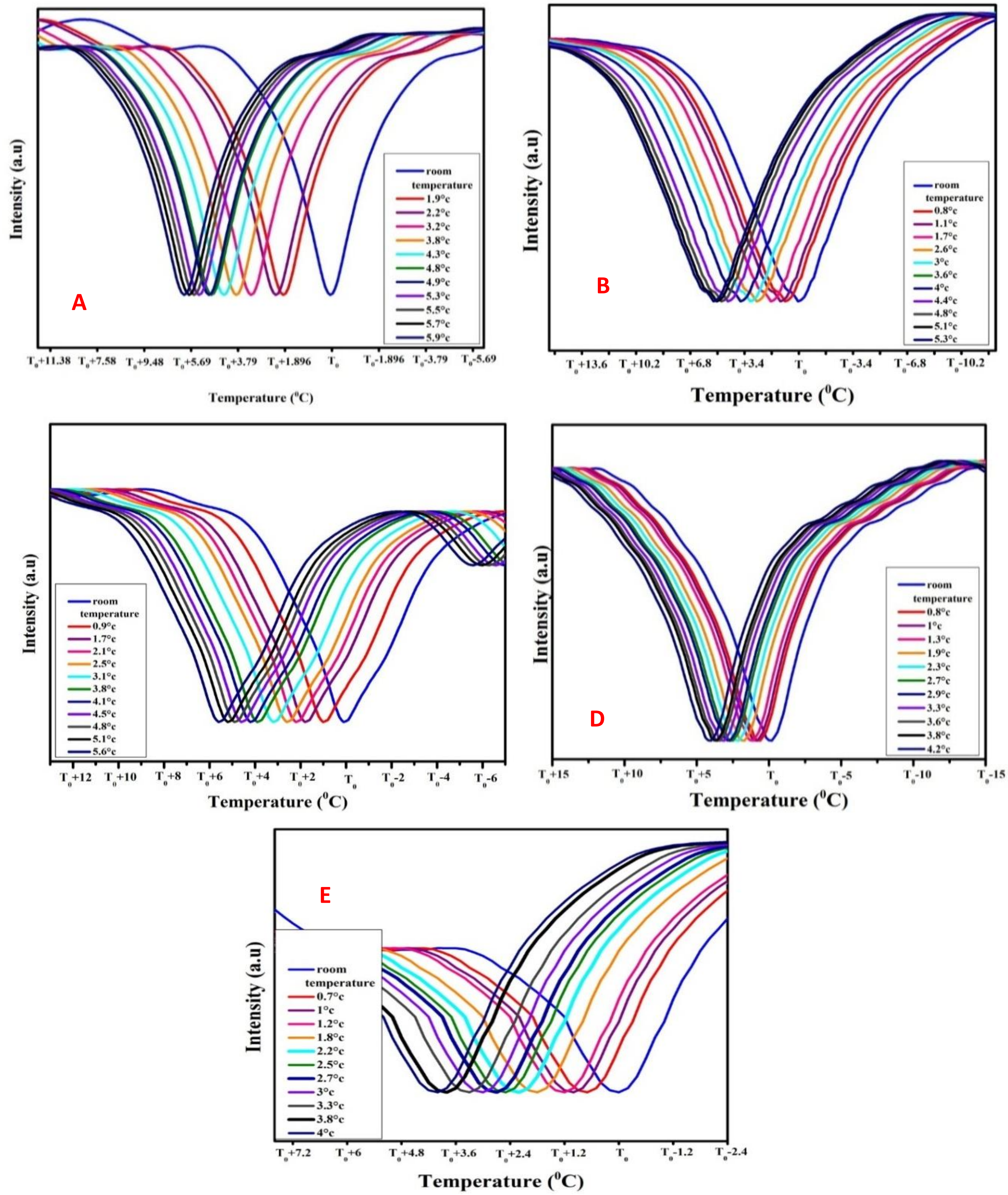

Fig. (3-2): Temperature increases examination after laser irradiation with Er,Cr:YSGG laser, (A) Enamel 1mm, (B) Enamel 2mm (C) Dentin 1 mm, (D) Dentin 2 mm, and (E) Dentin 3 mm

Throughout the ablation of enamel as well as dentine samples, heat generation was noticed. Enamel samples showed a larger increase in maximum temperature over dentine samples into general manner. Temperature elevation, on the other hand, was determined by the type as well as thickness of the related material. For dentin, the minimum temperature increase was noticed in the 3 mm group. Regarding enamel and dentin samples of 1mm, the entire rise was 4.3 ^{0}C, 3.4 ^{0}C over room temperature of 37 ^{0}C, respectively. The results are depicted in Fig (3-2).

3-1-2 Statistical Analysis

3-1-2-1 Statistical Analysis of Group 1 (temperature changes in samples irradiated with Nd:YAG laser).

The highest rise in temperature have been observed in the 1 mm thickness of the enamel sample (mean value of 5.59 ^{0}C), while the minimum temperature increase was observed in 3 mm thickness of dentin samples (mean value of 2.35 ^{0}C). Comparison of temperature increase between enamel samples of 1 mm and 2 mm thickness shows non-significant differences in temperatures ($p=0.115>0.05$). Comparison of temperature increase between dentin samples of 1, 2, and 3 mm thickness shows highly significant differences in temperature ($p=0.000 <0.05$). Generally, a comparison of temperature increase between enamel and dentin samples shows highly significant differences in variances ($p<0.05$).

Table (3-1): The statistical measurement for temperature increases under the effect of Nd: YAG laser.

Study groups Nd:YAG		Statistic	Std. Error	95% Confidence Interval	
				Lower	Upper
E1/ENAMEL samples1mm thickness	N	11		11	11
	Minimum	4.20			
	Maximum	7.60			
	Mean	5.5955	.34970	4.8892	6.2349
	Std. Deviation	1.1598		.41451	1.51137
	Variance	1.345		.174	2.284
E2/ ENAMEL samples 2mm thickness	N	11		11	11
	Minimum	3.00			
	Maximum	6.80			
	Mean	4.8164	.31848	4.1782	5.3906
	Std. Deviation	1.0562		.51228	1.55424
	Variance	1.116		.268	2.418
P value E1 vs e2	ANOVA= 2.65 / NS (0.115)				
D1/ DENTIN samples 1mm thickness	N	11		11	11
	Minimum	3.80			
	Maximum	7.90			
	Mean	5.4591 C	.49822	4.4507	6.2978
	Std. Deviation	1.65239		.56923	1.94758
	Variance	2.730		.343	3.793
D3/ DENTIN samples 2mm thickness	N	11		11	11
	Minimum	1.20			
	Maximum	5.10			
	Mean	3.2273 B	.39660	2.4765	3.8518
	Std. Deviation	1.3153		.56355	1.67544
	Variance	1.730		.318	2.808

D3/ DENTIN samples 3 mm thickness	**N**	11		11	11
	Minimum	1.50			
	Maximum	3.70			
	Mean	2.3591 A	.22124	1.9279	2.7970
	Std. Deviation	.73376		.34357	.95285
	Variance	.538		.123	.908
***P value D groups**	**ANOVA = 16.88 HS (0.000)**				
P value between all tested groups	**ANOVA = 14.986 HS (0.000)**				

* The letters A, B, and C for tested mean represented the levels of significant, highly significant start from the letter (A) and decreasing with the last one. Similar letters mean there are no significant differences between tested mean.

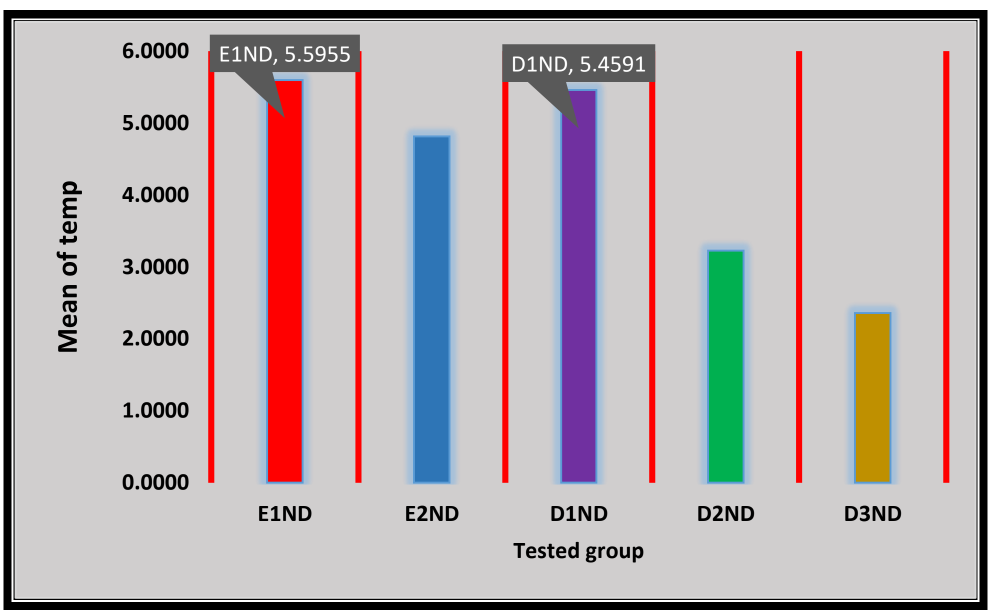

Fig. (3-3): Bar charts represent means temperature rise when Nd:YAG laser irradiate enamel and dentin samples.

3-1-2-2 Statistical Analysis of Group 2 (temperature changes in samples irradiated with Er,Cr:YSGG laser).

Means and standard deviations (SD) of maximum temperature values increase according to thickness of different dental hard tissues are shown in table (3-2). Generally, the enamel samples displayed a greater rise in maximum temperature than dentine samples. However, temperature rise depended on the thickness of the corresponding dental tissue.

Comparison of temperature increase between enamel samples of 1 mm and 2 mm thickness shows non-significant differences in temperatures ($p=0.115>0.05$). Comparison of temperature increase between dentin samples of 1, 2 and 3 mm thickness shows highly significant differences in temperature ($p=0.000 <0.05$). Generally, comparison of temperature increase between enamel and dentin samples shows highly significant differences in temperature. To compare the mean of different classes of groups, the collected data were analyzed using (ANOVA) test. Data were stated as mean and standard error (SE), with $p>0.05$ assumed statistically non-significant. Although $p<0.05$ and $<0.01,0.001$ were both considered significantly different. SPSS package (v 23/ France) was used to conduct the statistical analysis. For enamel and dentin dental specimens of 1 mm thick, mean temperature increase were 4.3 ^{0}C and 3.4 ^{0}C over ambient temperature of 37 ^{0}C, accordingly.

The temperature rises among enamel samples of 1 mm and 2 mm thickness indicates no statistically significant variations ($p=0.115>0.05$. In general, there are highly significant variations in variances ($p<0.05$) when comparing temperature rise among enamel and dentin specimens.

Table (3-2): The statistical measurement for temperature increases under the effect of Er,Cr:YSGG laser.

Study groups/ Erbium		Statistic	Std. Error	95% Confidence Interval Lower	95% Confidence Interval Upper
E1/ENAMEL samples1mm thickens	**N**	11		11	11
	Minimum	1.90			
	Maximum	5.90			
	Mean	4.3182	.41775	3.4727	4.9907
	Std. Deviation	1.3855		.77520	1.69865
	Variance	1.920		.601	2.885
E2/ ENAMEL samples 2mm thickness	**N**	11		11	11
	Minimum	.80			
	Maximum	5.30			
	Mean	3.3091	.48156	2.3366	4.1182
	Std. Deviation	1.5971		1.03627	1.91828
	Variance	2.551		1.074	3.680
P value E1 vs E2	**ANOVA = 2.51 / NS (P =0.29)**				
D1/ DENTIN samples 1mm thickness	**N**	11		11	11
	Minimum	.90			
	Maximum	5.50			
	Mean	3.4636	.45533	2.6091	4.2182
	Std. Deviation	1.5101		.97683	1.85368
	Variance	2.281		.954	3.436
D3/ DENTIN samples 2mm thickness	**N**	11		11	11
	Minimum	.80			
	Maximum	4.20			
	Mean	2.5273	.35164	1.8548	3.1000
	Std. Deviation	1.1662		.75416	1.40141
	Variance	1.360		.569	1.964

D3/ DENTIN samples 3 mm thickness	**N**	11		11	11
	Minimum	.70			
	Maximum	4.00			
	Mean	2.3818	.33678	1.7548	2.9455
	Std. Deviation	1.1169		.72916	1.35787
	Variance	1.248		.532	1.844
P value between D groups	**ANOVA = 2.33 /NS (P=0.115)**				
P value between all tested groups	**ANOVA = 3.6 HS (P=0.01)**				

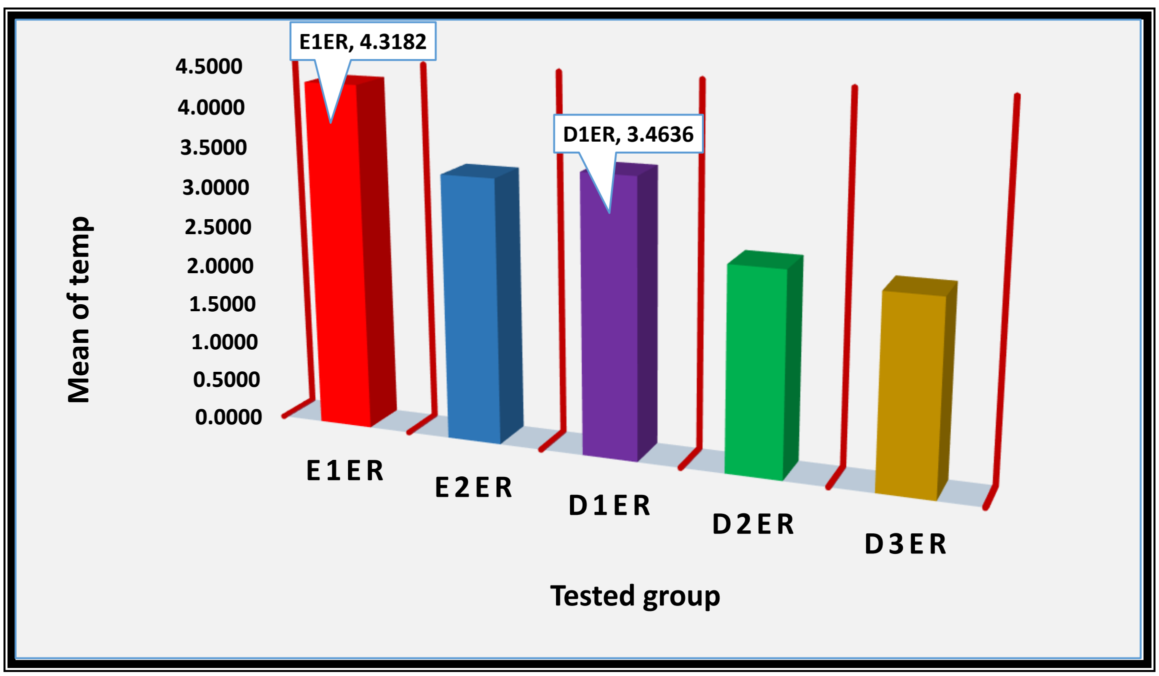

Fig. (3-4): Bar charts represent means temperature rise when Er,Cr:YSGG laser irradiate enamel and dentin samples.

3-1-2-3 Statistical Analysis Comparison Between Group 1 and 2

Comparison of temperature increases between group 1 and group 2 reveals significant differences in temperature between two groups of enamel samples of 1 mm thickness ($p=0.01<0.05$).

However, comparison between enamel samples of 2mm thickness show significant differences in temperature elevation between two groups ($p=0.09<0.05$).

Comparison between dentin samples of 1 mm thickness show significant differences in temperature elevation between the two groups ($p=0.003<0.05$), while comparison of temperature increases between dentin samples of 2 and 3 mm thickness shows non-significant differences in temperature between the two groups ($p>0.05$).

Table (3-3): comparison of statistical analysis between group 1 and 2

Study groups		**Statistic**	**Std. Error**	**Statistic**	**Std. Error**	**ANOVA**	**P value**
		Er,Cr:YSGG		**ND:YAG**			
E1	**N**	11		11			
	Mean	4.3182	.41775	5.5955	.34970	7.1	0.01
E2	**N**	11		11			
	Mean	3.3091	.48156	4.8164	.31848	8.1	0.009
D1	**N**	11		11			
	Mean	3.4636	.45533	5.4591	.49822	10.77	0.003
D2	**N**	11		11			
	Mean	2.5273	.35164	3.2273	.39660	1.8	0.186
D3	**N**	11		11			
	Mean	2.3818	.33678	2.3591	.22124	0.05	0.82

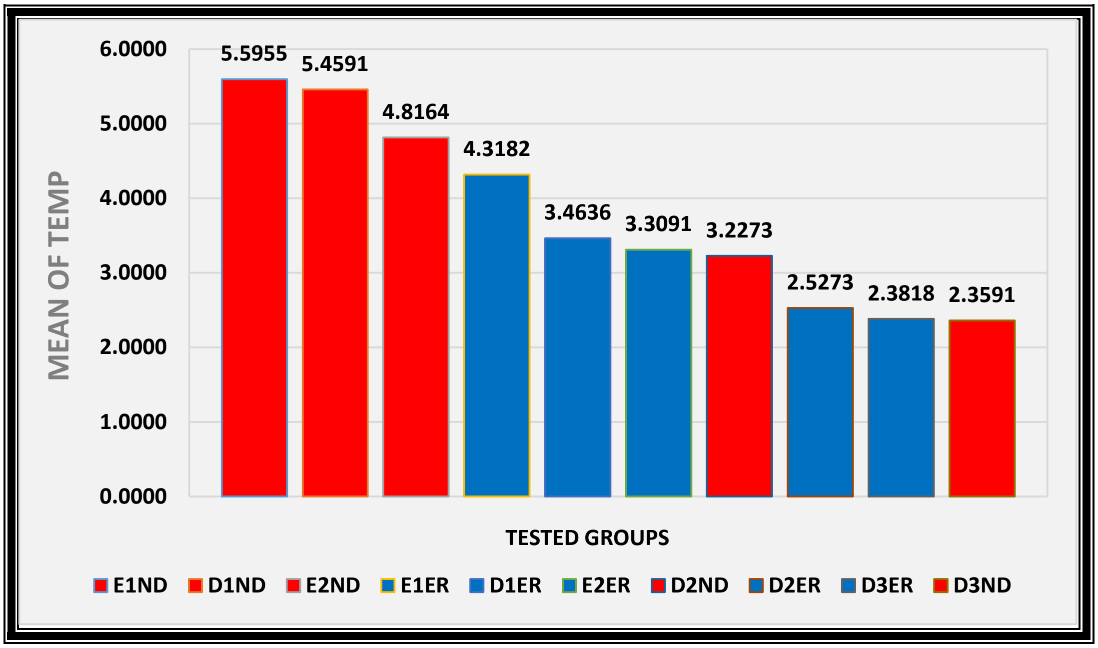

Fig. (3-5): Bar charts compare of temperature increases between group 1 and group 2.

In this study one-way ANOVA and two way anova were used: anova one way used for only one factor or independent variable, whereas there are two independent variables in a two-way ANOVA. In a one-way ANOVA, the one factor or independent variable analyzed has three or more categorical groups. A two-way ANOVA instead compares multiple groups of two factors

3-1-3 Surface Morphology

Morphological analysis and microstructure of the samples were examined under Atomic force microscopy (AFM).

Before to AFM examination, the enamel and dentin samples rinsed with deionized water and then left to dry. Enamel sample of 1mm thickness and dentin sample of 1 mm thickness were used in this study. All images possess topography images with a pixel resolution of 408×408. Topography images revealed surface and structure variations, while amplitude images allowed for a more detailed examination of surface characters and fine specifics. When all AFM images were compared, it was clear that afterward a high-potency treatment of laser, both of morphology and surface results were altered. Surface damage or pollution can dramatically affect average roughness (Sa), which represents the difference between highest and lowest points on a surface. The magnitude of average roughness for enamel and dentin samples irradiated by Nd:YAG and Er,Cr:YSGG is illustrated in table (3-4).

From magnitude of average roughness, one can deduce that the heat effect in enamel groups is more than in dentin group as a result of the difference in chemical structure between dentin and enamel.

3-1-3-1 Surface Morphology for Samples Irradiated with Nd:YAG Laser

Following irradiation of dental hard tissues, one sample from each group was studied under AFM to detect dental fractures, cracks, stains, carious, and other defects. Figure (3-6 a,b) represented the enamel group where the Sa are 29.1 nm.

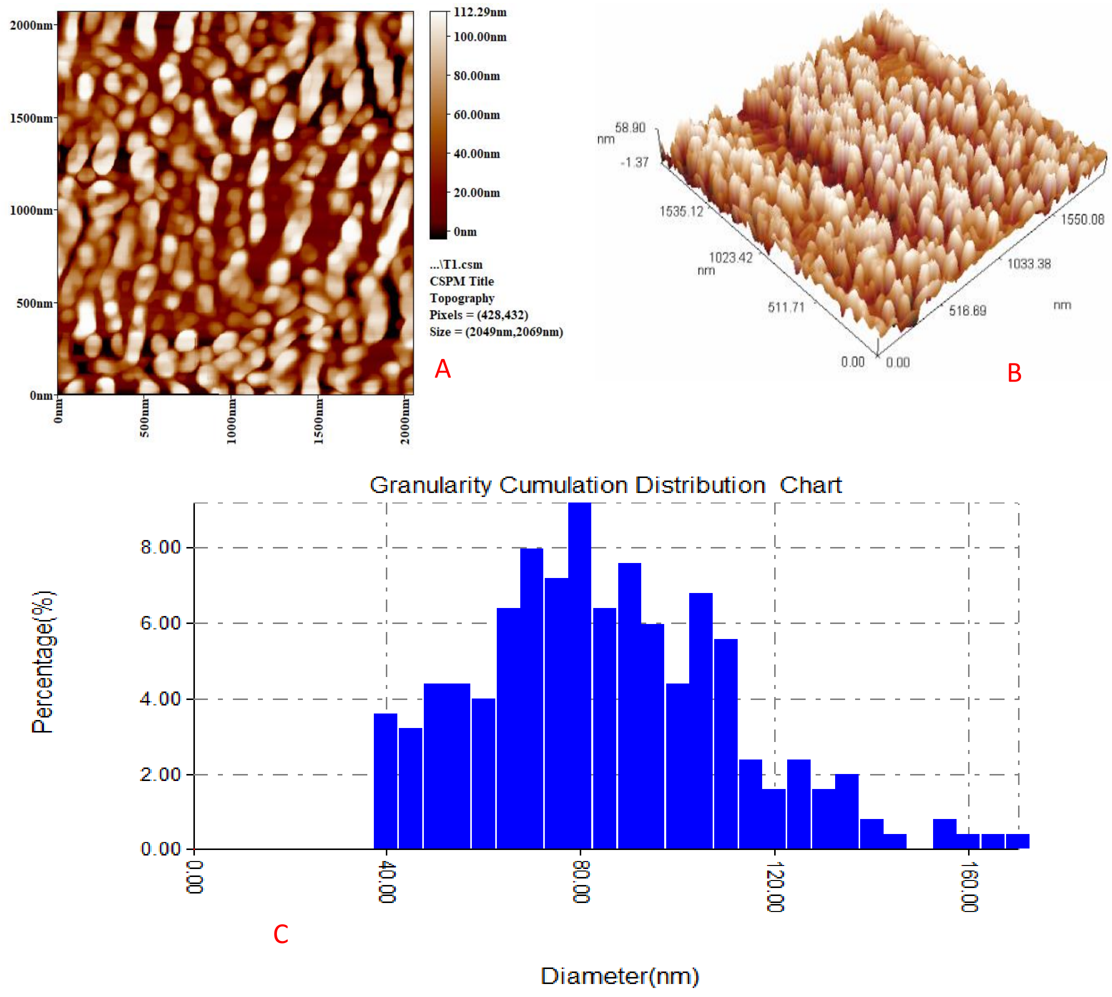

Fig. (3-6): AFM images for enamel tissue irradiated by Nd: YAG laser, (A) topography image (B) amplitude image (C) granularity chart.

Figure (3-7) represents dentinal tubules in addition to visible drafts caused by sample preparation. Dentinal tubules bounded via a wall (maybe produced by mechanical preparation of specimens) could be demonstrated in figure. (3-7) which reveals morphology of dentinal tubules as 3D image. Since dentin is highly vulnerable to dehydration, objects caused by shrinking cannot be completely avoided in operation. Figure (3-7) represented the dentin group where Sa is10.5 nm.

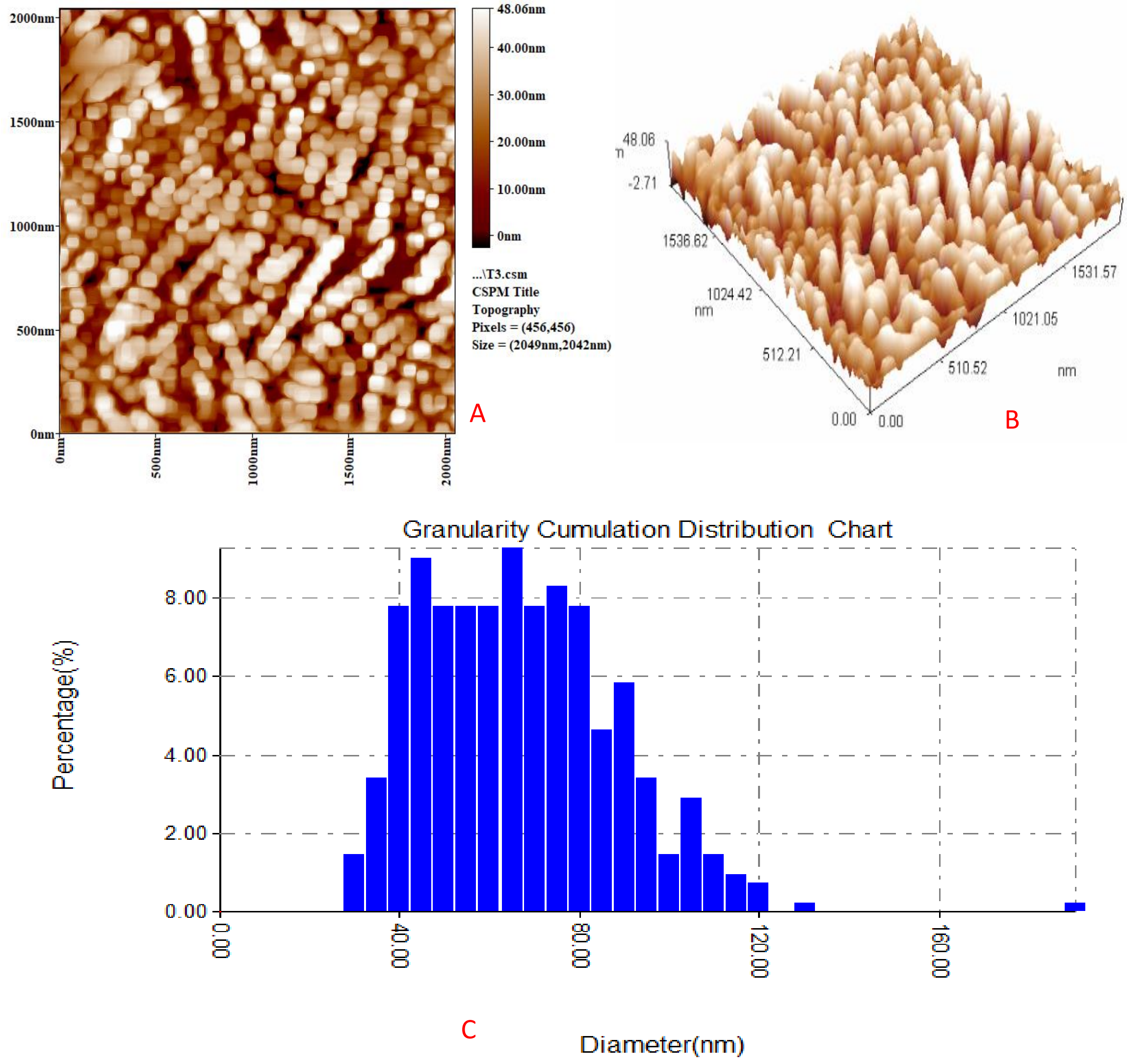

Fig. (3-7): AFM images for dentin tissue irradiated by Nd: YAG laser, (A) topography image (B) amplitude image (C) granularity chart.

3-1-3-2 Surface Morphology for Samples Irradiated with Er,Cr:YSGG Laser.

The same procedure used in the previous section, had been repeated for the samples that treated via Er,Cr:YSGG Laser. Figure (3-8 a,b) represented the enamel group where the Sa is 56.3 nm.

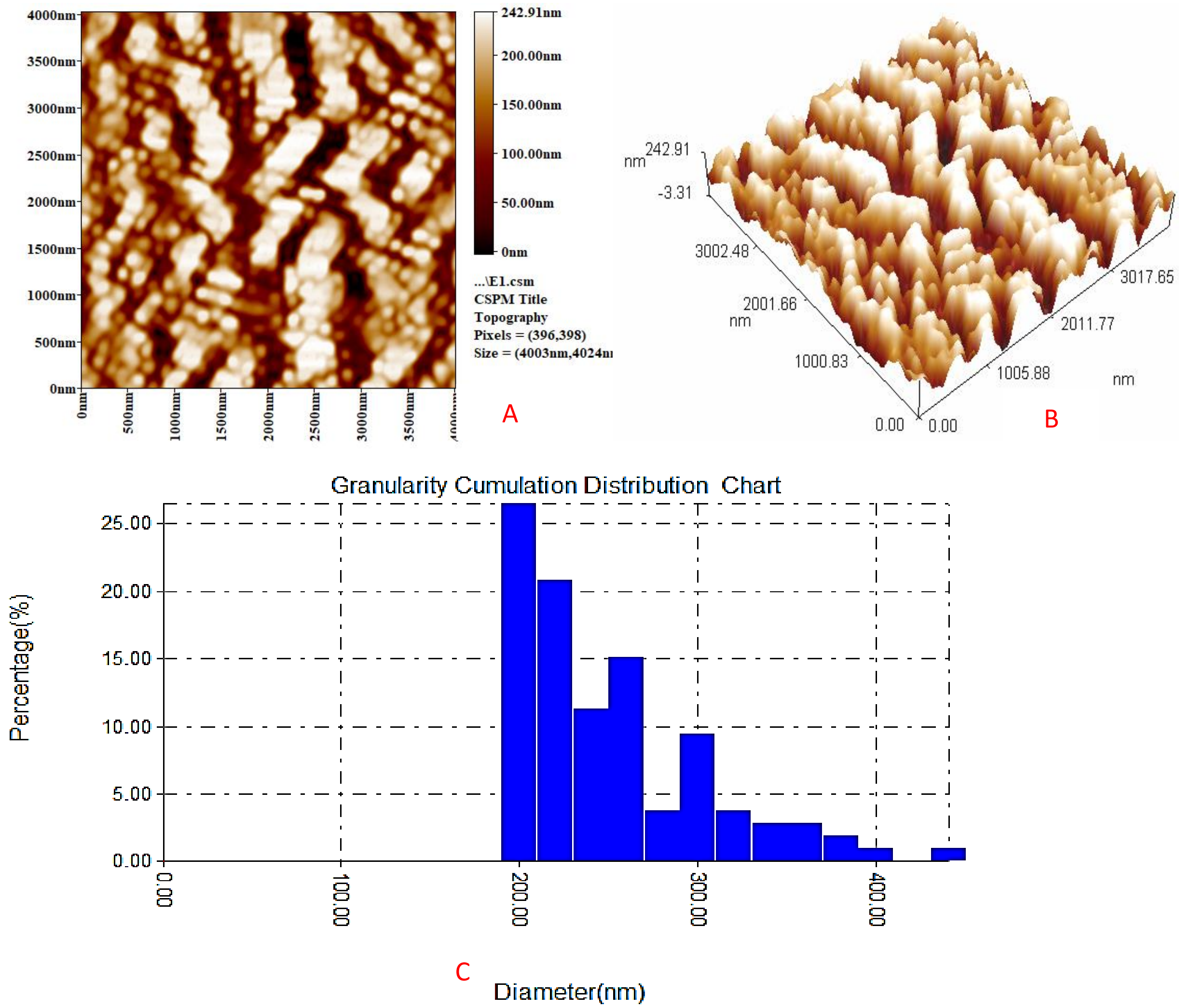

Fig. (3-8): AFM images for enamel tissue irradiated by Er,Cr:YSGG laser, (A) topography image (B) amplitude image (C) granularity chart.

Dentinal tubules as well as noticeable drafts generated when handling a specimen is also illustrated in figure (3-9). Dentinal tubules bounded via a wall (produced probably by mechanical preparation of the specimens) are observed in figure. (3-9). The incidence of artifacts triggered by shrinking can't be reduced in practice since dentin is intensely sensitive towards dehydration. Figure (3-9) represented the dentin group where the Sa is 35.3 nm.

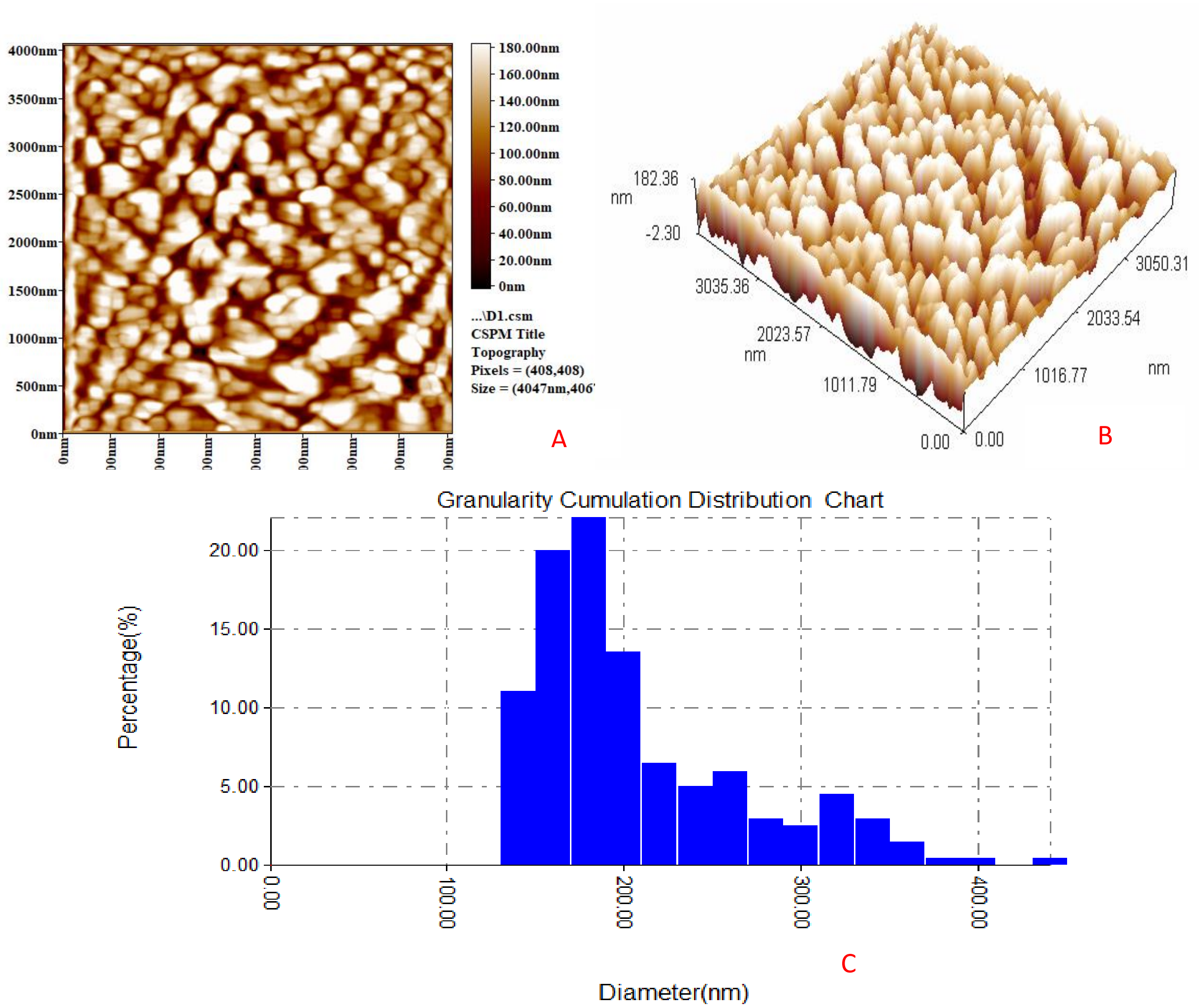

Fig. (3-9): AFM images for dentin tissue irradiated by Er,Cr:YSGG laser, (A) amplitude image (B) topography image (C) granularity chart.

Table (3-4): Average roughness (Sa) for enamel and dentin samples.

Sample	**Nd:YAG laser**	**Er,Cr:YSGG**
Enamel 1 mm thickness	Sa= 29.1 nm	Sa= 56.3 nm
Dentin 1mm thickness	Sa= 10.5 nm	Sa= 35.3 nm

3-1-4 Chemical Composition:

In the past few decades, Fourier transform infrared spectroscopy (FTIR) has been utilized widely for chemical description of inorganic materials (including the mineralized tissues). FTIR is a perfect method to examine the chemical composition belongings of biological materials, as the frequencies of numerous vibrational modes of inorganic and organic molecules are effective in the IR region. Enamel and dentin samples of 1 mm thickness were used in this study.

A Fourier transform infrared spectrometer is used to record the FTIR spectra. The spectra are assembled above the 400–4000 cm^{-1} range and zero fillings 4 cm^{-1}.

The peak position (cm^{-1}), peak intensity, and peak width (wide, medium, narrow) are so vital for band explanation. The tooth chemical composition is diverse from one tooth to other concerning overall organic matter and mineral matter. The peaks ascribed to enamel organic and mineral matters are illustrated in table (3-5), figure (3-10).

Dentin and enamel tissues are comprised of water, mineral and organic state. The water is appearing in two shapes: structural water, which is bound to the tissue powerfully, and adsorbed water, which is bound to the structure weakly. Covered with the wide H_2O absorptions, which the stretching vibration of the hydroxyl group of hydroxyapatite structure can be perceived at 3569 cm^{-1} in the carbonated apatite [144].

The mineral substance of the dental hard tissues is mostly comprised of calcium ions and phosphate that shape $Ca_{10}(PO_4)_5(OH)_2$ hydroxyapatite crystals, besides to magnesium, bicarbonate, potassium, citrate ions, and sodium with little quantities. These crystals vary in volume and amount for each mineralized tissue. The dentin organic matrix is essentially comprised of collagen- type I, and little amounts of other elements. But, the enamel organic matrix is minor, comprising proteolyzed fragments and an insoluble protein matrix allocated over the junction of dentin-enamel [144,145].

Phosphate ions possess 4-vibrational modes, namely υ_1, υ_2, υ_3, and υ_4. Whole these vibrational modes are infrared-active and perceived in both dentin and enamel tissues. Also, carbonate ions possess 4-vibrational modes, three of these are perceived in IR spectrum (υ_1, υ_2, and υ_3) and two of these are perceived in the Raman spectrum (υ_1, and υ_4). The carbonate υ_4-bands are rarely observed in the IR spectrum and further on possess extremely depressed

Table (3-5): The spectroscopic assignments and corresponded positions of various vibrational bands from FTIR spectra of human enamel.

Assignments	**Observed peaks (cm^{-1})**
PO_4^{-3}(υ_2)	484.13
PO_4^{-3}(υ_4)	561.29
PO_4^{-3}(υ_4)	603.72
CO_3^{-2} (υ_2)	875.68
PO_4^{-3} (υ_3)	1043.5
CO_3^{-2} (υ_3)	1402.25
CO_3^{-2} (υ_4)	1454.33
CO_3^{-2} (υ_3) + amide II	1541.42
Carbonate + H_2O + Amide I	1633.71
Structural OH^{-1}+ amide B: COH / Stretching mode	2924.09
Structural OH^{-1}+ amide B: COH / Stretching mode	3441.01

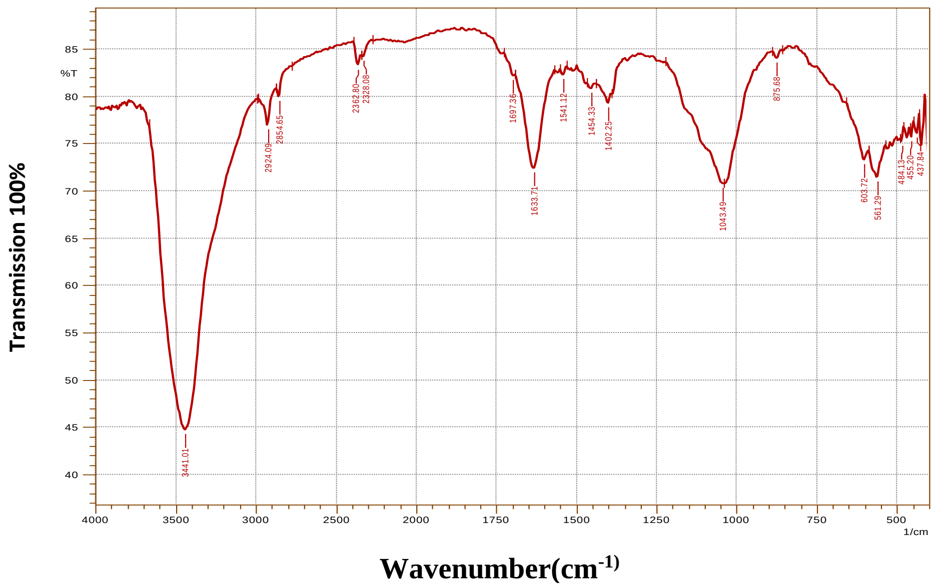

Fig. (3-10): FTIR spectra for un lased enamel samples.

While the peaks ascribed to dentin tissue are illustrated in table (3-6), figure (3-11).

Table (3-6): The spectroscopic assignments and corresponded positions of various vibrational bands from FTIR spectra of human dentin

Assignments	Detected valleys (cm^{-1})
$PO_4^{-3}(\upsilon_1)$	470.63
$PO_4^{-3}(\upsilon_2)$	600–550
$PO_4^{-3}(\upsilon_3)$	1033.85
$CO_3^{-2}(\upsilon_3)$ overlapped with collagen	1454
H_2O + Amide I/ C=O stretching	1641

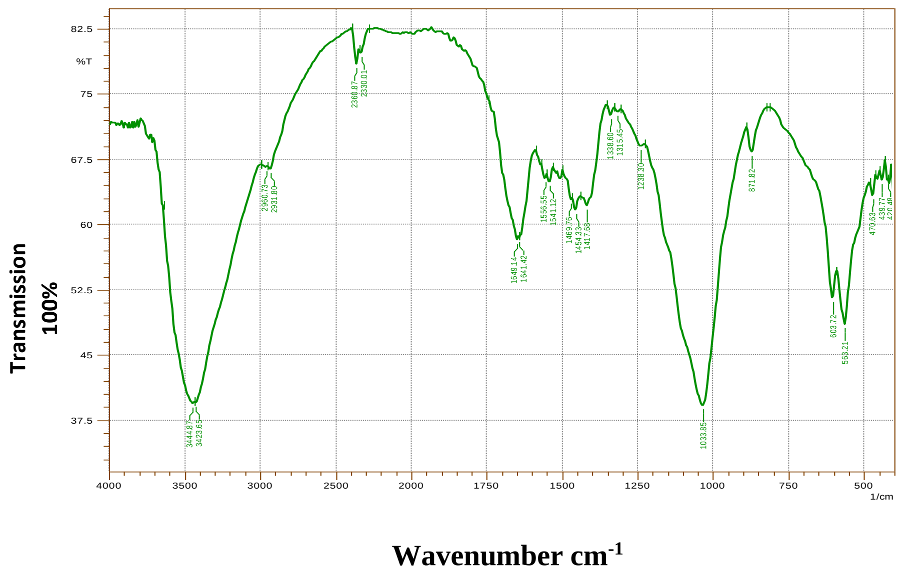

Fig. (3-11): FTIR spectra for un lased dentin samples.

3-1-4-1 Chemical Composition for Samples Irradiated with Nd:YAG Laser

FTIR spectra of enamel samples irradiated with 1.064 μm laser are displays in figure (3-12) and Table (3-7). The peaks 3424 cm^{-1} and 2999 cm^{-1} which have intensity locations 27.994 and 44.819, are related to the hydroxyl (OH^{-1}) group, and amide B: COH, respectively. The peak around 1638 cm^{-1} related to the organic matrix which means the teeth possess carbonate and amide I. While, the peak of 1549 cm^{-1} associated with amide II. The peaks corresponded with carbonate (υ_3) are around 1460 cm^{-1}, 1415 cm^{-1}, the peak corresponded with carbonate (υ_2) is around and 874 cm^{-1}. The peaks related to phosphate ions (υ_1, υ_2, υ_3, υ_4, υ_5) vibrations located at 470 cm^{-1}, 565 cm^{-1}, 605 cm^{-1}, and 1038 cm^{-1} and 1092 cm^{-1}. Compare with previous works, no change is perceived in phosphate matter due to it is greatest stable content in mineralized tissues. The reduction in carbonate and water contents is accredited to thermal influence in laser-tissue interaction.

Table (3-7): The spectroscopic assignments and corresponded positions of various vibrational bands from FTIR spectra of human enamel for group 1

Assignments	Observed peaks (cm^{-1})
$PO_4^{-3}(\upsilon_2)$	470
$PO_4^{-3}(\upsilon_4)$	565
$PO_4^{-3}(\upsilon_4)$	605
CO_3^{-2} (υ_2)	873.75
PO_4^{-3} (υ_3)	1037.7
PO_4^{-3} (υ_3)	1091.75
CO_3^{-2} (υ_3)	1415.75
CO_3^{-2} (υ_4)	1460.11
CO_3^{-2} (υ_3) + amide II	1548.84
Carbonate + H_2O + Amide I	1637.56
Structural OH^{-1}+ amide B: COH / Stretching mode	2999.21
Structural OH^{-1}+ amide B: COH / Stretching mode	3423.65

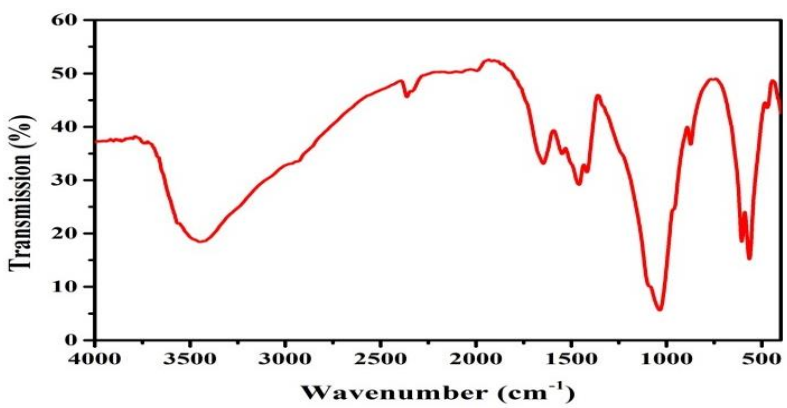

Fig. (3-12): FTIR spectra for enamel after the irradiation with Nd:YAG laser.

While in the case of dentin tissue, FTIR spectra are displayed in figure (3-13) and table (3-8). The greatest intense peaks corresponded to PO_4^{-3} (υ_1, υ_2, υ_3) vibrations were antisymmetric stretching mode at 1036 cm^{-1} (υ_3 band) and 600–550 cm^{-1} antisymmetric bending mode related to υ_2 band, while the peak around 467 cm^{-1} related to υ_1 band. The 1641 cm^{-1} and 1458 cm^{-1} are related to absorption bands of OH^{-1} and CO_3^{-2} (υ_3), respectively.

Table (3-8): The spectroscopic assignments and corresponded positions of various vibrational bands from FTIR spectra of human dentin for group 1

Assignments	Detected valleys (cm^{-1})
$PO_4^{-3}(\upsilon_1)$	467
$PO_4^{-3}(\upsilon_2)$	600–550
$PO_4^{-3}(\upsilon_3)$	1036
CO_3^{-2} (υ_3) overlapped with collagen	1458
H_2O + Amide I/ C=O stretching	1641

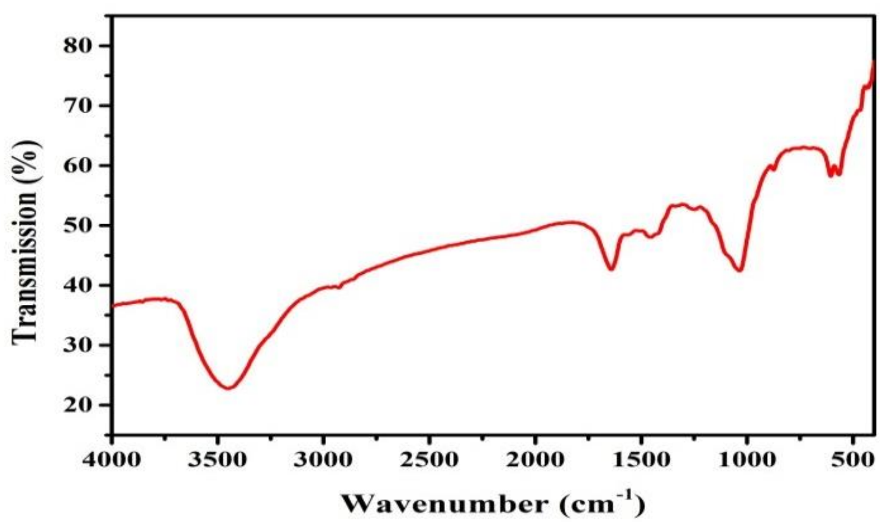

Fig. (3-13): FTIR spectra for dentin after the irradiation with Nd:YAG laser.

3-1-4-2 Chemical composition for Samples Irradiated with Er,Cr:YSGG Laser

The transmission spectra of FTIR that are regarded to enamel samples irradiated by 2.78 μm source are displays in figure (3-14) and Table (3-9).

The peaks 3424 cm^{-1} and 2999 cm^{-1} which have intensity locations 27.994 and 44.819 are related to the hydroxyl (OH^{-1}) group, and amide B: COH, respectively. The peak around 1638 cm^{-1} related to the organic matrix which means the teeth possess carbonate and amide I. While, the peak of 1549 cm^{-1} associated with amide II. The peaks corresponded with carbonate (υ_3) are around 1460 cm^{-1}, 1415 cm^{-1}, the peak corresponded with carbonate (υ_2) is around and 874 cm^{-1}. The peaks related to phosphate ions (υ_1, υ_2, υ_3, υ_4, υ_5) vibrations located at 470 cm^{-1}, 565 cm^{-1}, 605 cm^{-1}, and 1038 cm^{-1} and 1092 cm^{-1}. Compare with un lased samples, no change is perceived in phosphate matter due to its greatest steady content in mineralized matters. The reduction in carbonate and water contents is accredited to thermal influence in laser-tissue interaction.

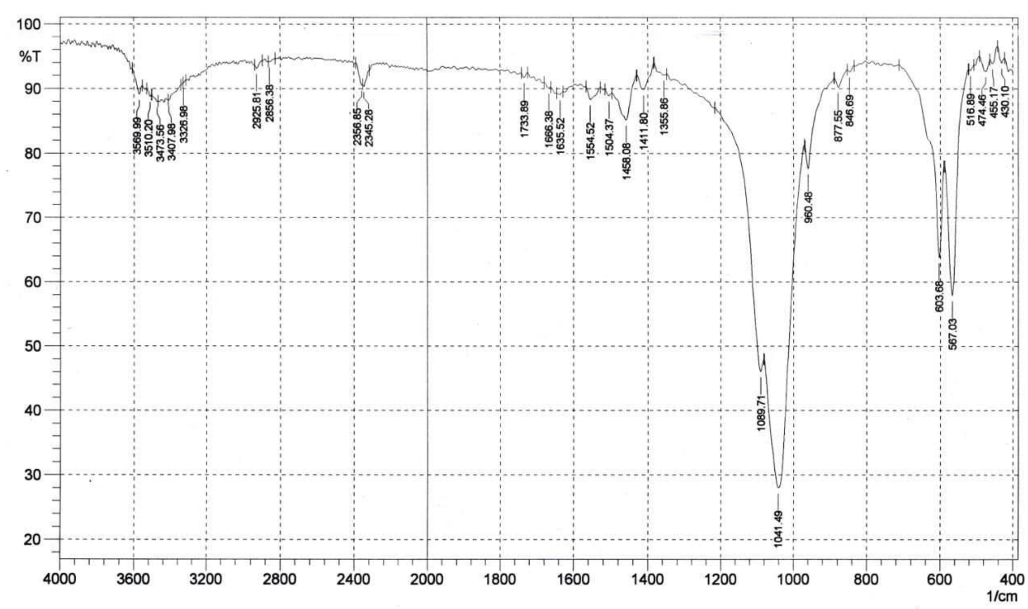

Fig. (3-14): FTIR spectra for enamel after the irradiation with Er,Cr:YSGG laser.

Table (3-9): The spectroscopic assignments and corresponded positions of various vibrational bands from FTIR spectra of human enamel for group 2

Assignments	Detected valleys (cm^{-1})
$PO_4^{-3}(\upsilon_2)$	470
$PO_4^{-3}(\upsilon_4)$	567
$PO_4^{-3}(\upsilon_4)$	603
$CO_3^{-2}(\upsilon_2)$	873.75
B-type carbonate	877
$PO_4^{-3}(\upsilon_1)$ Symmetric stretching	960
PO_4^{-3} (υ_3) Antisymmetric stretching	1040
PO_4^{-3} (υ_3)	1089
$CO_3^{-2}(\upsilon_3)$	1411
CO_3^{-2} (υ_3) Antisymmetric stretching	1450–1550 1544
$CO_3^{-2}(\upsilon_4)$ Symmetric angular deformation	1458
C-N stretching vibrations	1554
Carbonate + H_2O + Amide I C=O stretching	1635
H_2O + Amide I	1690–1650 1700–1600 1666
CO_3	2300–2400
Amide B: COH	2925
Structural OH	3448, 3569

While in the case of dentin tissue, FTIR spectra are displayed in figure (3-15) and Table (3-10).

Table (3-10): The spectroscopic assignments and corresponded positions of various vibrational bands from FTIR spectra of human dentin for group 2

Assignments	Detected valleys (cm^{-1})
B-type carbonate	875
A-type carbonate	894
PO_4^{3-} v_1	960
PO_4^{-3} (v_3)	1039.6
CO_3^{2-} v_3 overlapped with collagen	1410–1560 1450–1640 (43)
CO_3^{-2} (v_3)	1415
Scissoring CH_2	1450
CO_3^{-2} (v_4)	1458
CO_3^{-2} (v_3) + amide II	1548.84
CNH	1500–1600 (39)
Carbonate + H_2O + Amide I	1637.5
Adsorbed H_2O (v_2)	1640
C-O stretching	1630-1650
H_2O v_2 overlap by the collagen band	1660
CO_3	2300–2400
Structural OH	3300–3600
hydroxyapatite, and amide N–H stretch	3436
Structural OH^{-1}+ amide B: COH / Stretching mode	3421.5
CO_3	2300–2400
Structural OH^{-1}+ amide B: COH / Stretching mode	3421.5

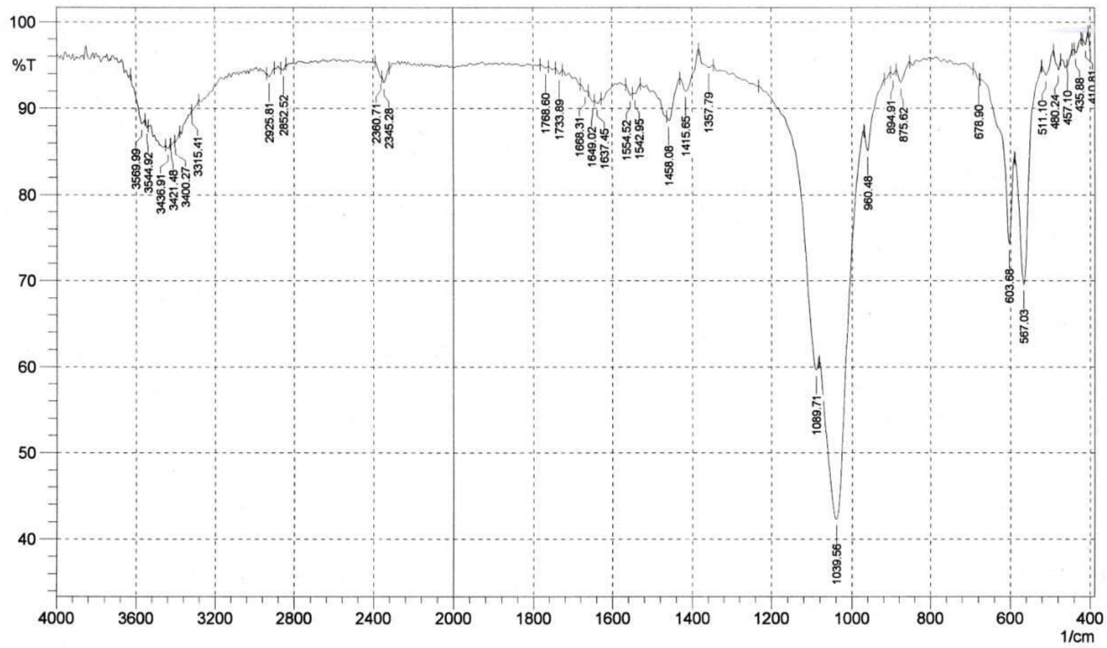

Fig. (3-15): FTIR spectra for dentin after the irradiation with Er,Cr:YSGG laser.

3-2 Discussion

Heat production throughout laser ablation may produce permanent damage to the dental pulp, aching sensations may happen throughout laser ablation adjacent to pulpal tissues. So, controlling the temperature elevation is a must. In this study, an instantaneous approach to measure the temperature of the ablated dental hard tissues experimentally using a novel technique based on an optical fiber sensor (fast detector) has been designed fabricated and tested .Traditional temperature sensors like thermocouples suffer from different drawbacks such as relatively low accuracy of temperature measurements, nonlinearity of a conversion characteristic and necessity to take into account the temperature of reference junctions and low sensitivity. So, the current technique of temperature measurement is a step forward in applying a new approach to avoid all unwanted side effects due to heat elevation throughout laser radiation [146].

In this, in vitro study to measure temperature elevation via laser ablation process, non-carious extracted premolar human teeth were equally grouped into two major groups of five subgroups each. Each subgroup was composed of 11 samples. The major groups consist of two groups which were representing temperature variation during Nd:YAG as well as Er,Cr:YSGG lasers cavity preparation.

Two different lasers, namely Q-switched Nd:YAG laser and Er,Cr:YSGG have been used to perform the experiments .

The 1.064 μm wavelength of the Nd:YAG laser processes less absorption in comparison to Erbium and CO_2 lasers. Nevertheless, the short pulse duration (9 ns) can accelerate the ablation process contrary to the Erbium free-running laser. The current in vitro study has considered the use of laser with its unique features as a heat source.

While, Er,Cr:YSGG laser produces photons that possess wavelength of 2.78 μm which are strongly absorbed via water as well as hydroxyapatite (the two principal components of tooth structure) [79]. Absorbed energy induces vaporization of water and makes micro-explosions of hard tissue [147]. Micro-explosions of irradiated tissues result in micro fragmentation, which is eliminated by high pressure induced by steam. Temperature elevation is a direct consequence of this process which also may explain the temperature difference among Er:Cr:YSGG and Nd:YAG groups. This result come agrees well with the reults of the previously published work by Cavalcanti et al [31] and Armengol et al. [148].

Air-water spray cooling is essential in high-speed tooth preparation, regardless of the pressure applied or type of bur associated with the equipment [150,151]. However, more water spray will decrease significantly the efficiency of laser dental ablation. On the other hand, increased intra-pulpal temperature was believed to be due to reduced dental hard tissue thicknesses. This will provide the laser operator or dentist with much higher flexibility for maneuvering.

Experimental characterization of tooth heat transfer can be divided into two main types: in vivo and in vitro. In vivo characterization is desirable since it can reflect the active processes (e.g., blood circulation in pulp chamber and fluid motion in dentinal tubules [45,46,152] not captured in vitro [152]. However, in view of the challenges of in vivo tests, in vitro tests are also widely used. Existing in vitro characterization of tooth heat transfer can be divided into three categories depending on how the contribution of pulpal tissue to the tooth thermal behavior is modeled (e.g., with empty pulpal chamber [154,155], with simulated pupal tissue [63,156], with consideration of microcirculation [156]. In vitro heat transfer studies have been carried out in tooth with empty pulp chamber (pulp soft tissue was extracted) [154,155]. However, in this case, the measured temperature change on pulpal wall does not necessarily indicate the temperature change in pulp soft tissue, as the thermal conductivity and heat capacity of teeth with empty pulp chambers are significantly different from those with filled chambers [157].

Of course, heat diffusion and accumulation depends mainly on the thermal and optical properties of the tooth. Namely, the thermal conductivity and diffusivity of enamel and dentine. Human dentin, enamel, and dental cements have thermal diffusivities of 2.04×10^{-3}, 3.22×10^{-3}, and 0.99-1.87×10^{-3} cm^2/sec, respectively. The corresponding thermal conductivities are 1.36×10^{-3}, 1.84×10^{-3}, and 0.50-1.51×10^{-3} cal/cm.sec. [33,159,160]. One important issue concerning the above tooth thermal properties is the thermal relaxation time and its relation with laser pulse width. This fact needs more extensive investigation to check out how much the amount of the removal of deposited heat in tooth constitutes for successful cavity preparation.

When hard dental tissues are exposed to laser beam, the temperature rises to a specific point where the pulp is damaged. In 1965, Zach and Cohen found that temperature increase in the pulp at about 5.6 °C resulted in a loss of pulp vitality (15 percent of teeth tested) [64]. On the other side, ref. [160] reported that the thermal agitation in the range of 39–42 ^{0}C causes hyperemia in the rat central pulp. Heat generation of 44 ^{0}C and higher resulted in RBC accumulation. Also preserving the temperatures in the range of 46-50 ^{0}C for interval 30 s, causing coagulation and the cessation of circulating blood. In general, a temperature increase of more than 5.6 ^{0}C was found to produce permanent harm in the pulpal tissue. A fast response (1 ms) fiber sensor was stuck at the back of the teeth. This sensor gives true readings in a short time and consequently can provide feedback to reduce the laser energy to avoid any possible damage to the pulp due to excessive heat generation.

Generally, enamel specimens exhibited a larger increase in temperature than dentine tissues during laser-tissue interaction process as a result of the difference in chemical structure between dentin and enamel.

In 1mm enamel specimens, maximum mean temperature achieved during Nd:YAG laser treatment was (5.59 ^{0}C), compared to (4.3 ^{0}C) for specimens irradiated via Er,Cr:YSGG. Temperatures below 5.6 ^{0}C are deemed non-threatening to pulp tissue [64]. Nevertheless, Er,Cr:YSSG laser demonstrated a superior results than Nd:YAG laser.

The highest temperature increase was seen in the cavity preparation with laser radiation of Nd: YAG laser was achieved in enamel samples of 1 mm thickness. All other tested samples showed a little bit lesser temperature increase. In the current study, a mean temperature rises to 5.59 ^{0}C could be detected in a 1mm thickness enamel irradiated with Nd:YAG laser. Nevertheless, this does not reflect the total amount of thermal energy dissipated in the pulp tissue Additionally, another therapeutically essential aspect that must be considered is the temperature rise, which can be influenced by pulp microcirculation. Simulating an artificially blood microcirculation with a constant flow of water in within pulp chamber was tested the influence of numerous light curing units on damp samples [161]. Although the temperatures rise during enamel ablation was higher than for dentin ablation, the path to the pulp is shorter in dentin, and pulp survival is more at risk from dentin warming [163,164].

The thickness of the remaining dentin plays an important role in protection against thermal injuries of the pulp. Although dentin has a low thermal conductivity, pulpal damage risk is potentially higher due to the increasing tubular surface area, especially in deeper restorations [164]. For this reason, the critical dentin thickness for deep cavities was selected to simulate the deep cavity preparation in clinical situations.

The current investigation found that when remaining dentin thickness decreased, pulpal temperature increased. Because it is impossible to determine the residual dentin thicknesses in vivo, the operator must select appropriate laser parameters for ablation of sound or carious dental tissue. Based on clinical expertise and other parameters including size of the tooth as well as the region to be treated, thus the operator must assess the remaining dentin thickness and also modify the laser settings. There were some changes in tooth morphology, structure of the dentin, pulp cavity dimensions, and position. This could explain why the temperatures of the teeth tested are different [150].

Despite the large temperature spike caused by tooth preparation into this in vitro investigation, slower or quicker rises and drops in temperature might not be associated with pulpal injury, because the temperature values findings in this research cannot be directly translated to temperature variations in vivo, Heat conduction inside the tooth was not included in the current study's experimental approach. In addition, the surrounding periodontal tissues can promote heat dissipation in vivo, limiting the intrapulpal temperature rise [29].

The morphology evaluations of the lased surfaces of the dental samples revealed a small presence of the Carbone portion, indicating that the laser therapy was able to photo-effect and effectively treat the structure surfaces, according to the findings of the current in vitro analysis. Our findings showed that when infrared laser was used in conjunction with unique protocol and criteria, it produced successful outcomes. The rise in temperature throughout laser radiation exposure suggested that the energy transmitted was insufficient to cause morphological harm to the dental specimen surface. All temperature rise measurements are far below the 10 ^{0}C threshold for periodontal tissue damage. As a result, these results support the protocol's protection in the periodontium

A combination of a highly sensitive fiber sensor with high flexibility to monitor temperature elevation during the dental cavity preparation may pave for establishing a well-defined and forward cavity preparation procedure. This will reduce or even eliminate any pulpal vitality problems as well giving more access to the operator (dentist).

3-3 Conclusions:

1- All class 1 cavity preparations via Nd:YAG laser and Er,Cr:YSGG laser causes elevation in intrapulpal temperature.

2- Nd:YAG laser cavity preparation without water cooling produced highest temperature elevation among three subgroups(enamel 1mm thickness, dentin 1mm thickness, enamel 2mm thickness), which regarded threaten to dental pulp.

3- Er,Cr:YSGG laser cavity preparation water cooling produced less temperature elevation in comparison with Nd:YAG laser, which produces less insult to dental pulp.

4- Increasing the cavity depth; decreasing remaining dentin thickness resulted in higher intrapulpal temperature for Nd:YAG laser.

5- An innovative technique of temperature measurement using an optical fiber sensor that possesses fast response time has been employed for instant measurement of temperature rises in dental tissues after laser radiation.

3-4 Future works:

1- Further histopathological study of pulp tissue is needed to evaluate cavities prepared with Er,Cr:YSGG laser and Nd:YAG laser.

2- Further in vitro study is required to evaluate the effect of different laser parameter on intrapulpal temperature.

3- Further investigations as SEM, EDS are required to evaluate the possible changes in the tooth surface structure that may occur due to the thermal effects generated during cavity preparation.

References:

[1] M. Ahmed, C. L. Brace, F. T. Lee Jr, and S. N. Goldberg, “Principles of and advances in percutaneous ablation,” *Radiology*, vol. 258, no. 2, pp. 351–369, 2011.

[2] E. Schena, D. Tosi, P. Saccomandi, E. Lewis, and T. Kim, “Fiber optic sensors for temperature monitoring during thermal treatments: An overview,” *Sensors (Switzerland)*, vol. 16, no. 7. Multidisciplinary Digital Publishing Institute, p. 1144, 2016, doi: 10.3390/s16071144.

[3] K. Onseng *et al.*, “Beneficial effects of adjuvant melatonin in minimizing oral mucositis complications in head and neck cancer patients receiving concurrent chemoradiation,” *J. Altern. Complement. Med.*, vol. 23, no. 12, pp. 957–963, 2017.

[4] J. S. Young and J. W. Simmons, “Chemotherapeutic medications and their emergent complications,” *Emerg. Med. Clin.*, vol. 32, no. 3, pp. 563–578, 2014.

[5] P. Mohammadazari, “Application of Capacitive Temperature Sensors for Food Processing Applications.” Southern Illinois University at Edwardsville, 2018.

[6] S. Nammour *et al.*, “Safety parameters for pulp temperature during selective ablation of caries by KTP laser in vitro,” *J. Clin. Laser Med. Surg.*, vol. 22, no. 2, pp. 99–104, 2004.

[7] D. YU, G. L. POWELL, W. I. HIGUCHI, and J. L. FOX, “Comparison of three lasers on dental pulp chamber temperature change,” *J. Clin. Laser Med. Surg.*, vol. 11, no. 3, pp. 119–122, 1993.

[8] W. S. Brown, W. A. Dewey, and H. R. Jacobs, “Thermal properties of

teeth," *J. Dent. Res.*, vol. 49, no. 4, pp. 752–755, 1970.

[9] D. Zhang, J. Wang, Y. Wang, and X. Dai, "A fast response temperature sensor based on fiber Bragg grating," *Meas. Sci. Technol.*, vol. 25, no. 7, p. 75105, 2014.

[10] D. Niu *et al.*, "High-resolution and fast-response optical waveguide temperature sensor using asymmetric Mach-Zehnder interferometer structure," *Sensors Actuators A Phys.*, vol. 299, p. 111615, 2019.

[11] Y. Zhao, Q. Wu, and Y. Zhang, "Theoretical analysis of high-sensitive seawater temperature and salinity measurement based on C-type micro-structured fiber," *Sensors Actuators B Chem.*, vol. 258, pp. 822–828, 2018.

[12] Y. Qian, Y. Zhao, Q. Wu, and Y. Yang, "Review of salinity measurement technology based on optical fiber sensor," *Sensors Actuators B Chem.*, vol. 260, pp. 86–105, 2018.

[13] Y. Bao, Y. Huang, M. S. Hoehler, and G. Chen, "Review of fiber optic sensors for structural fire engineering," *Sensors*, vol. 19, no. 4, p. 877, 2019.

[14] J. M. López-Higuera, L. R. Cobo, A. Q. Incera, and A. Cobo, "Fiber optic sensors in structural health monitoring," *J. Light. Technol.*, vol. 29, no. 4, pp. 587–608, 2011.

[15] F. Urban, J. Kadlec, R. Vlach, and R. Kuchta, "Design of a pressure sensor based on optical fiber Bragg grating lateral deformation," *Sensors*, vol. 10, no. 12, pp. 11212–11225, 2010.

[16] D. Kowal, W. Urbanczyk, and P. Mergo, "Twin-Core Fiber-Based Mach Zehnder Interferometer for Simultaneous Measurement of Strain and

Temperature,” *Sensors*, vol. 18, no. 3, p. 915, 2018.

[17] Q. Yao *et al.*, “Simultaneous measurement of refractive index and temperature based on a core-offset Mach–Zehnder interferometer combined with a fiber Bragg grating,” *Sensors Actuators A Phys.*, vol. 209, pp. 73–77, 2014.

[18] E. Udd and W. B. Spillman Jr, *Fiber optic sensors: an introduction for engineers and scientists*. John Wiley & Sons, 2011.

[19] M. Y. Mohd Noor *et al.*, “High Sensitivity of Balloon-Like Bent MMI Fiber Low-Temperature Sensor,” *IEEE Photonics Technol. Lett.*, vol. 27, no. 18, pp. 1989–1992, 2015, doi: 10.1109/LPT.2015.2448944.

[20] D. I. A.-J. and A. S. and A. H. Al-Janabi, “High sensitivity balloon-like thermometric sensor based on bent single mode fiber,” *Meas. Sci. Technol.*, 2020.

[21] X. Liu, Y. Zhao, R.-Q. Lv, and Q. Wang, “High sensitivity balloon-like interferometer for refractive index and temperature measurement,” *IEEE Photonics Technol. Lett.*, vol. 28, no. 13, pp. 1485–1488, 2016.

[22] P. A. Ana, A. Blay, W. Miyakawa, and D. M. Zezell, “Thermal analysis of teeth irradiated with Er, Cr: YSGG at low fluences,” *Laser Phys. Lett.*, vol. 4, no. 11, p. 827, 2007.

[23] A. Uhl, A. Völpel, and B. W. Sigusch, “Influence of heat from light curing units and dental composite polymerization on cells in vitro,” *J. Dent.*, vol. 34, no. 4, pp. 298–306, 2006.

[24] G. R. Martins, B. N. Cavalcanti, and S. M. Rode, “Increases in intrapulpal temperature during polymerization of composite resin,” *J. Prosthet. Dent.*, vol. 96, no. 5, pp. 328–331, 2006.

[25] A. D. Vanderlei, A. L. S. Borges, B. N. Cavalcanti, and S. M. Rode, “Ultrasonic versus high-speed cavity preparation: analysis of increases in pulpal temperature and time to complete preparation,” *J. Prosthet. Dent.*, vol. 100, no. 2, pp. 107–109, 2008.

[26] M. Fahey, O. Onyejekwe, H. L. Mason, and K. Mitra, “Precise dental ablation using ultra-short-pulsed 1552 nm laser,” *Int. J. Heat Mass Transf.*, vol. 51, no. 23–24, pp. 5732–5739, 2008.

[27] S. D. Spitz, “Lasers in prosthodontics: clinical realities of a dental laser in a prosthodontic practice,” *Alpha Omegan*, vol. 4, no. 101, pp. 188–194, 2008.

[28] A. Uhl, R. W. Mills, and K. D. Jandt, “Polymerization and light-induced heat of dental composites cured with LED and halogen technology,” *Biomaterials*, vol. 24, no. 10, pp. 1809–1820, 2003.

[29] M. Hannig and B. Bott, “In-vitro pulp chamber temperature rise during composite resin polymerization with various light-curing sources,” *Dent. Mater.*, vol. 15, no. 4, pp. 275–281, 1999.

[30] S. Bouillaguet, G. Caillot, J. Forchelet, M. Cattani-Lorente, J. C. Wataha, and I. Krejci, “Thermal risks from LED-and high-intensity QTH-curing units during polymerization of dental resins,” *J. Biomed. Mater. Res. Part B Appl. Biomater. An Off. J. Soc. Biomater. Japanese Soc. Biomater. Aust. Soc. Biomater. Korean Soc. Biomater.*, vol. 72, no. 2, pp. 260–267, 2005.

[31] B. N. Cavalcanti, C. Otani, and S. M. Rode, “High-speed cavity preparation techniques with different water flows,” *J. Prosthet. Dent.*, vol. 87, no. 2, pp. 158–161, 2002.

[32] B. N. Cavalcanti, J. L. Lage-Marques, and S. M. Rode, “Pulpal temperature increases with Er: YAG laser and high-speed handpieces,” *J. Prosthet. Dent.*, vol. 90, no. 5, pp. 447–451, 2003.

[33] M. Lin, F. Xu, T. J. Lu, and B. F. Bai, “A review of heat transfer in human tooth-Experimental characterization and mathematical modeling,” *Dent. Mater.*, vol. 26, no. 6, pp. 501–513, 2010, doi: 10.1016/j.dental.2010.02.009.

[34] D. A. Sumikawa, G. W. Marshall, L. Gee, and S. J. Marshall, “Microstructure of primary tooth dentin,” *Pediatr. Dent.*, vol. 21, no. 7, pp. 439–444, 1999.

[35] C. Carda and A. Peydro, “Ultrastructural patterns of human dentinal tubules, odontoblasts processes and nerve fibres,” *Tissue Cell*, vol. 38, no. 2, pp. 141–150, 2006.

[36] D. H. Pashley, “Dynamics of the pulpo-dentin complex,” *Crit. Rev. Oral Biol. Med.*, vol. 7, no. 2, pp. 104–133, 1996.

[37] R. M. Frank, “Ultrastructure of human dentine 40 years ago—progress and perspectives,” *Arch. Oral Biol.*, vol. 44, no. 12, pp. 979–984, 1999.

[38] C. Hildebrand, K. Fried, F. Tuisku, and C. S. Johansson, “Teeth and tooth nerves,” *Prog. Neurobiol.*, vol. 45, no. 3, pp. 165–222, 1995.

[39] R. Orchardson and S. W. Cadden, “An update on the physiology of the dentine–pulp complex,” *Dent. Update*, vol. 28, no. 4, pp. 200–209, 2001.

[40] A. NANCI, “Enamel: composition, formation, and structure,” *Ten Cate’s oral Histol. Dev. Struct. Funct.*, pp. 141–190, 2008.

[41] H. Haskan, T. Boyraz, and M. A. Kilicarslan, “Investigation of thermal

stresses in dental restoration by mathematical method," *J. Eur. Ceram. Soc.*, vol. 27, no. 2–3, pp. 899–902, 2007.

[42] H. E. Goodis, V. Winthrop, and J. M. White, "Pulpal responses to cooling tooth temperatures," *J. Endod.*, vol. 26, no. 5, pp. 263–267, 2000.

[43] A. Kishen, U. Ramamurty, and A. Asundi, "Experimental studies on the nature of property gradients in the human dentine," *J. Biomed. Mater. Res.*, vol. 51, no. 4, pp. 650–659, 2000.

[44] E. P. Tunc, "Finite element analysis of heat generation from different light-polymerization sources during cementation of all-ceramic crowns," *J. Prosthet. Dent.*, vol. 97, no. 6, pp. 366–374, 2007.

[45] B. Öztürk, A. Üşümez, A. N. Öztürk, and F. Ozer, "In vitro assessment of temperature change in the pulp chamber during cavity preparation," *J. Prosthet. Dent.*, vol. 91, no. 5, pp. 436–440, 2004.

[46] P. Linsuwanont, J. E. A. Palamara, and H. H. Messer, "An investigation of thermal stimulation in intact teeth," *Arch. Oral Biol.*, vol. 52, no. 3, pp. 218–227, 2007.

[47] M. F. de Magalhaes, R. A. N. Ferreira, P. A. Grossi, and R. M. de Andrade, "Measurement of thermophysical properties of human dentin: effect of open porosity," *J. Dent.*, vol. 36, no. 8, pp. 588–594, 2008.

[48] O. Feuerstein, K. Zeichner, C. Imbari, Z. Ormianer, N. Samet, and E. I. Weiss, "Temperature changes in dental implants following exposure to hot substances in an ex vivo model," *Clin. Oral Implants Res.*, vol. 19, no. 6, pp. 629–633, 2008.

[49] S. Matalon, H. Slutzky, N. Wassersprung, I. Goldberg-Slutzky, and A.

Ben-Amar, “Temperature rises beneath resin composite restorations during curing.,” *Am. J. Dent.*, vol. 23, no. 4, pp. 223–226, 2010.

[50] L. Zach, “Pulp response to externally applied heat,” *Oral surg Oral med Oral pathol*, vol. 19, pp. 515–530, 1965.

[51] P. Baldissara, S. Catapano, and R. Scotti, “Clinical and histological evaluation of thermal injury thresholds in human teeth: a preliminary study,” *J. Oral Rehabil.*, vol. 24, no. 11, pp. 791–801, 1997.

[52] C. M. Sturdevant, T. M. Roberson, E. J. Swift, and H. Heymann, *Sturdevant’s Art & Science of Operative Dentistry*. Mosby, 2002.

[53] L. Ceballos, R. Osorio, M. Toledano, and G. W. Marshall, “Microleakage of composite restorations after acid or Er-YAG laser cavity treatments,” *Dent. Mater.*, vol. 17, no. 4, pp. 340–346, 2001.

[54] M. T. Schein, J. S. Bocangel, G. E. C. Nogueira, and P. A. L. Schein, “SEM evaluation of the interaction pattern between dentin and resin after cavity preparation using Er: YAG laser,” *J. Dent.*, vol. 31, no. 2, pp. 127–135, 2003.

[55] A. A. Al-Qudah, C. A. Mitchell, P. A. Biagioni, and D. L. Hussey, “Effect of composite shade, increment thickness and curing light on temperature rise during photocuring,” *J. Dent.*, vol. 35, no. 3, pp. 238–245, 2007.

[56] I. Özkoçak, M. M. Taşkan, H. Göktürk, F. Aytaç, and E. Karaarslan, “Temperature increases on the external root surface during endodontic treatment using single file systems,” *Niger. J. Clin. Pract.*, vol. 18, no. 5, pp. 676–680, 2015, doi: 10.4103/1119-3077.158976.

[57] J. J. Sauk, K. Norris, R. A. Foster, J. M. Moehring, and M. J. Somerman,

"Expression of heat stress proteins by human periodontal ligament cells," *J. Oral Pathol. Med.*, vol. 17, no. 9-10, pp. 496–498, 1988.

[58] S. E. Line, A. M. Polson, and H. A. Zander, "Relationship between periodontal injury, selective cell repopulation and ankylosis," *J. Periodontol.*, vol. 45, no. 10, pp. 725–730, 1974.

[59] F. Atrizadeh, J. Kennedy, and H. Zander, "Ankylosis of teeth following thermal injury," *J. Periodontal Res.*, vol. 6, no. 3, pp. 159–167, 1971.

[60] L. Firoozmand, R. Faria, M. A. Araujo, R. Di Nicoló, and M. F. Huthala, "Temperature rise in cavities prepared by high and low torque handpieces and Er:YAG laser," *Br. Dent. J.*, vol. 205, no. 1, pp. 3–6, 2008, doi: 10.1038/sj.bdj.2008.491.

[61] V. Srimaneepong, J. Palamara, and P. Wilson, "Pulpal space pressure and temperature changes from Nd: YAG laser irradiation of dentin White star," *J. Dent.*, vol. 30, pp. 291–296, Sep. 2002, doi: 10.1016/S0300-5712(02)00023-4.

[62] T. F. Watson, D. Flanagan, and D. G. Stone, "High and low torque handpieces: Cutting dynamics, enamel cracking and tooth temperature," *Br. Dent. J.*, vol. 188, no. 12, pp. 680–686, 2000, doi: 10.1038/sj.bdj.4800576.

[63] D. C. Attrill, R. M. Davies, T. A. King, M. R. Dickinson, and A. S. Blinkhorn, "Thermal effects of the Er: YAG laser on a simulated dental pulp: a quantitative evaluation of the effects of a water spray," *J. Dent.*, vol. 32, no. 1, pp. 35–40, 2004.

[64] L. Zach and G. Cohen, "Pulp response to externally applied heat," *Oral Surgery, Oral Med. Oral Pathol.*, vol. 19, no. 4, pp. 515–530, 1965, doi:

10.1016/0030-4220(65)90015-0.

[65] R. M. Love, “The Effects of Laser Irradiation of the Dental Tissues--A Review,” *N. Z. Dent. J.*, vol. 91, no. 406, pp. 134–137, 1995.

[66] S. Chopra and H. M. Chawla, *Lasers in Chemical and Biological Sciences: Winter School: Revised Papers*. Wiley Eastern Limited, 1992.

[67] A. K. Murray and M. R. Dickinson, “Investigation into the interaction of a XeCl Excimer laser with hard tissue,” in *Laser-Tissue Interaction XI: Photochemical, Photothermal, and Photomechanical*, 2000, vol. 3914, pp. 137–143.

[68] J. S. Nelson and M. W. Berns, “Basic laser physics and tissue interactions,” *Contemp Dermatol*, vol. 2, pp. 3–15, 1988.

[69] K. Johar and J. Kirpa, *Fundamentals of laser dentistry*. JP Medical Ltd, 2011.

[70] M. H. Niemz, *Laser-tissue interactions*. Springer, 2007.

[71] D. J. Coluzzi, “Fundamentals of dental lasers: science and instruments,” *Dent. Clin.*, vol. 48, no. 4, pp. 751–770, 2004.

[72] L. Casagrande, R. Brayner, J. S. Barata, and F. B. de Araujo, “Cervical microleakage in composite restorations of primary teeth—in vitro study,” *J. Dent.*, vol. 33, no. 8, pp. 627–632, 2005.

[73] D. M. Clarkson, “Lasers in dentistry.,” *Dent. Update*, vol. 19, no. 3, pp. 115–116, 1992.

[74] “Laser Safety Handbook,” no. February, pp. 17–18, 2011.

[75] D. H. Sliney and J. Mellerio, *Safety with lasers and other optical sources: a comprehensive handbook*. Springer Science & Business

Media, 2013.

[76] D. N. Dederich and R. D. Bushick, “Lasers in dentistry: separating science from hype,” *J. Am. Dent. Assoc.*, vol. 135, no. 2, pp. 204–212, 2004.

[77] C. R. dos Santos, M. R. Tonetto, C. D. Presoto, M. C. Bandeca, O. B. Oliviera Jr, and S. Calabrez-Filho, “Application of Er: YAG and ER, Cr: YSGG Lasers in cavity preparation for dental tissues: A literature review,” *World J Dent*, vol. 3, no. 4, pp. 340–343, 2012.

[78] R. Hibst and U. Keller, “Effects of water spray and repetition rate on the temperature elevation during Er: YAG laser ablation of dentine,” in *Medical Applications of Lasers III*, 1996, vol. 2623, pp. 139–144.

[79] P. A. Ana, L. Bachmann, and D. M. Zezell, “Lasers effects on enamel for caries prevention,” *Laser Phys.*, vol. 16, no. 5, pp. 865–875, 2006.

[80] R. Hibst, “Lasers for Caries Removal and Cavity Preparation: State of the Art and Future Directions.,” *J. Oral Laser Appl.*, vol. 2, no. 4, 2002.

[81] A. Aoki, K. M. Sasaki, H. Watanabe, and I. Ishikawa, “Lasers in nonsurgical periodontal therapy,” *Periodontol. 2000*, vol. 36, no. 1, pp. 59–97, 2004.

[82] D. T. Chimello-Sousa, A. E. de Souza, M. A. Chinelatti, J. D. Pécora, R. G. Palma-Dibb, and S. A. M. Corona, “Influence of Er: YAG laser irradiation distance on the bond strength of a restorative system to enamel,” *J. Dent.*, vol. 34, no. 3, pp. 245–251, 2006.

[83] R. J. Freiberg and C. D. Cozean, “Pulsed erbium laser ablation of hard dental tissue: the effects of atomized water spray versus water surface film,” in *Lasers in dentistry VIII*, 2002, vol. 4610, pp. 74–84.

[84] L. J. Walsh, “The current status of laser applications in dentistry,” *Aust. Dent. J.*, vol. 48, no. 3, pp. 146–155, 2003.

[85] J. Clark, A. L. Symons, S. Diklic, and L. J. Walsh, “Effectiveness in diagnosing residual caries with various methods during cavity preparation using conventional methods, chemo-mechanical caries removal, and Er: YAG laser.,” *Aust. Dent. J.*, vol. 46, no. 4, pp. S20–S20, 2001.

[86] C. B. Gimbel, “Hard tissue laser procedures.,” *Dent. Clin. North Am.*, vol. 44, no. 4, pp. 931–953, 2000.

[87] Y. Ando, A. Aoki, H. Watanabe, and I. Ishikawa, “Bactericidal effect of erbium YAG laser on periodontopathic bacteria,” *Lasers Surg. Med. Off. J. Am. Soc. Laser Med. Surg.*, vol. 19, no. 2, pp. 190–200, 1996.

[88] R. Hibst, K. Stock, R. Gall, and U. Keller, “Controlled tooth surface heating and sterilization by Er: YAG laser radiation,” in *Laser Applications in Medicine and Dentistry*, 1996, vol. 2922, pp. 119–126.

[89] A. Mehl, M. Folwaczny, C. Haffner, and R. Hickel, “Bactericidal effects of 2.94 µm Er: YAG-laser radiation in dental root canals,” *J. Endod.*, vol. 25, no. 7, pp. 490–493, 1999.

[90] E. S. Bornstein and M. A. Lomke, “The safety and effectiveness of dental Er: YAG lasers. A literature review with specific reference to bone,” *Dent. Today*, vol. 22, no. 10, pp. 129–133, 2003.

[91] S. Nammour and C. Nyssen-Behets, “Increased resistance to artificial caries-like lesions in dentin treated with CO2 laser,” *Caries Res.*, vol. 26, no. 3, pp. 170–175, 1992.

[92] D. E. Schuller, “Use of the laser in the oral cavity.,” *Otolaryngol. Clin.*

North Am., vol. 23, no. 1, pp. 31–42, 1990.

[93] P. Wilder-Smith *et al.*, “Morphological effects of ArF excimer laser irradiation on enamel and dentin,” *Lasers Surg. Med. Off. J. Am. Soc. Laser Med. Surg.*, vol. 20, no. 2, pp. 142–148, 1997.

[94] Y. Tokita, M. Sunakawa, and H. Suda, “Pulsed Nd: YAG laser irradiation of the tooth pulp in the cat: I. Effect of spot lasing,” *Lasers Surg. Med. Off. J. Am. Soc. Laser Med. Surg.*, vol. 26, no. 4, pp. 398–404, 2000.

[95] H. C. Midgley 3rd, “Nd: YAG contact laser surgery. The scalpel of the future?,” *Otolaryngol. Clin. North Am.*, vol. 23, no. 1, pp. 99–105, 1990.

[96] L. J. Miserendino, G. C. Levy, E. Abt, and I. M. Rizoiu, “Histologic effects of a thermally cooled Nd: YAG laser on the dental pulp and supporting structures of rabbit teeth,” *Oral surgery, oral Med. oral Pathol.*, vol. 78, no. 1, pp. 93–100, 1994.

[97] P. N. R. Nair, M. M. Baltensperger, H. Luder, and G. K. H. Eyrich, “Pulpal response to Er: YAG laser drilling of dentine in healthy human third molars,” *Lasers Surg. Med.*, vol. 32, no. 3, pp. 203–209, 2003.

[98] J. Neev, K. Pham, J. P. Lee, and J. M. White, “Dentin ablation with three infrared lasers,” *Lasers Surg. Med. Off. J. Am. Soc. Laser Med. Surg.*, vol. 18, no. 2, pp. 121–128, 1996.

[99] I. W. M. Jeffrey, B. Lawrenson, E. M. Saunders, and C. Longbottom, “Dentinal temperature transients caused by exposure to CO2 laser irradiation and possible pulpal damage,” *J. Dent.*, vol. 18, no. 1, pp. 31–36, 1990.

[100] D. A. Stewardson, A. C. C. Shortall, E. Harrington, and P. J. Lumley,

"Thermal changes and cure depths associated with a high intensity light activation unit," *J. Dent.*, vol. 32, no. 8, pp. 643–651, 2004, doi: https://doi.org/10.1016/j.jdent.2004.06.007.

[101] A. Shortall, W. El-Mahy, D. Stewardson, O. Addison, and W. Palin, "Initial fracture resistance and curing temperature rise of ten contemporary resin-based composites with increasing radiant exposure," *J. Dent.*, vol. 41, no. 5, pp. 455–463, 2013, doi: https://doi.org/10.1016/j.jdent.2013.02.002.

[102] E. Asmussen and A. Peutzfeldt, "Temperature rise induced by some light emitting diode and quartz-tungsten-halogen curing units," *European Journal of Oral Sciences*, vol. 113, no. 1. pp. 96–98, 2005, doi: 10.1111/j.1600-0722.2004.00181.x.

[103] N. Hofmann, B. Hugo, and B. Klaiber, "Effect of irradiation type (LED or QTH) on photo-activated composite shrinkage strain kinetics, temperature rise, and hardness.," *European journal of oral sciences*, vol. 110, no. 6. pp. 471–479, 2002, doi: 10.1034/j.1600-0722.2002.21359.x.

[104] J. Leprince, J. Devaux, T. Mullier, J. Vreven, and G. Leloup, "Pulpal-temperature rise and polymerization efficiency of LED curing lights," *Oper. Dent.*, vol. 35, no. 2, pp. 220–230, 2010, doi: 10.2341/09-203-L.

[105] E. M. da Silva, A. G. Penelas, M. S. Simão, J. D. N. Filho, L. T. Poskus, and J. G. A. Guimarães, "Influence of the degree of dentine mineralization on pulp chamber temperature increase during resin-based composite (RBC) light-activation," *J. Dent.*, vol. 38, no. 4, pp. 336–342, 2010, doi: 10.1016/j.jdent.2009.12.007.

[106] C. J. Kleverlaan and A. J. De Gee, "Curing efficiency and heat generation of various resin composites cured with high-intensity halogen

lights," *European Journal of Oral Sciences*, vol. 112, no. 1. pp. 84–88, 2004, doi: 10.1111/j.0909-8836.2004.00101.x.

[107] A. A. Al-Qudah, C. A. Mitchell, P. A. Biagioni, and D. L. Hussey, "Thermographic investigation of contemporary resin-containing dental materials," *J. Dent.*, vol. 33, no. 7, pp. 593–602, 2005, doi: https://doi.org/10.1016/j.jdent.2005.01.010.

[108] H. S. Chang *et al.*, "Thermal analysis of bulk filled composite resin polymerization using various light curing modes according to the curing depth and approximation to the cavity wall," *J. Appl. Oral Sci.*, vol. 21, no. 4, pp. 293–299, 2013, doi: 10.1590/1678-775720130036.

[109] B. S. Lee, J. H. Jeng, C. P. Lin, S. Shoji, and W.-H. Lan, "Thermal effect and morphological changes induced by Er: YAG laser with two kinds of fiber tips to enlarge the root canals," *Photomed. Laser Surg.*, vol. 22, no. 3, pp. 191–197, 2004.

[110] C. Wu, H. Y. Fu, K. K. Qureshi, B.-O. Guan, and H.-Y. Tam, "High-pressure and high-temperature characteristics of a Fabry–Perot interferometer based on photonic crystal fiber," *Opt. Lett.*, vol. 36, no. 3, pp. 412–414, 2011.

[111] L. Zhao, B. Liu, Y. Wu, T. Sun, Y. Mao, and T. Nan, "Measurement of refractive index and temperature using balloon-shaped Mach-Zehnder interferometer," *Optik (Stuttg).*, vol. 188, pp. 115–119, 2019.

[112] G. P. Agrawal, *Fiber-optic communication systems*, vol. 222. John Wiley & Sons, 2012.

[113] K. A. Fidanboylu and H. S. Efendioglu, "Fiber optic sensors and their applications," in *5th International Advanced Technologies Symposium*

(IATS'09), 2009, vol. 6, pp. 2–3.

[114] N. H. Yusof, H. A. Razak, H. Arof, and S. W. Harun, "Performance comparison of high temperature sensor based on non-adiabatic silica microfiber and single mode-multimode-single mode fiber structure," *Microw. Opt. Technol. Lett.*, vol. 61, no. 2, pp. 431–435, 2019.

[115] G. LEO, N. AEBY, and D. INAUDI, "Medical apparatus system having optical fiber load sensing capability," 2012.

[116] A. D. Kersey, "Optical fiber sensors for permanent downwell monitoring applications in the oil and gas industry," *IEICE Trans. Electron.*, vol. 83, no. 3, pp. 400–404, 2000.

[117] Y. Zhao, X. Li, X. Zhou, and Y. Zhang, "Review on the graphene based optical fiber chemical and biological sensors," *Sensors Actuators B Chem.*, vol. 231, pp. 324–340, 2016.

[118] O. S. Wolfbeis, "Fluorescence optical sensors in analytical chemistry," *TrAC Trends Anal. Chem.*, vol. 4, no. 7, pp. 184–188, 1985.

[119] H. Alsweefe, S. K. Al-Hayali, and A. H. M. Al-Janabi, "Efficient humidity sensor based on an etched no-core fiber coated with copper oxide nanoparticles," *J. Nanophotonics*, vol. 12, no. 4, p. 46018, 2018.

[120] É. Pinet, "Fabry-Pérot fiber-optic sensors for physical parameters measurement in challenging conditions," *J. sensors*, vol. 2009, 2009.

[121] H. S. Efendioglu, T. Yildirim, and K. Fidanboylu, "Prediction of force measurements of a microbend sensor based on an artificial neural network," *Sensors*, vol. 9, no. 9, pp. 7167–7176, 2009.

[122] A. M. S. and A. A.-J. Dunia I. Al-Janabi, "High sensitivity balloon-like thermometric sensor based on bent single mode fiber," *Meas. Sci.*

Technol., 2020, doi: https://doi.org/10.1088/1361-6501/ab9458.

[123] S. K. Al-Hayali, A. M. Salman, and A. H. Al-Janabi, “Effect of hygroscopic polymer-coatings on the performance of relative humidity sensor based on macro-bend single-mode fiber,” *Opt. Fiber Technol.*, vol. 62, p. 102460, 2021.

[124] Y. Zhao, Y. Peng, M. Chen, and R.-J. Tong, “Humidity sensor based on unsymmetrical U-shaped microfiber with a polyvinyl alcohol overlay,” *Sensors Actuators B Chem.*, vol. 263, pp. 312–318, 2018.

[125] J. Mathew, Y. Semenova, and G. Farrell, “A fiber bend based humidity sensor with a wide linear range and fast measurement speed,” *Sensors Actuators A Phys.*, vol. 174, pp. 47–51, 2012.

[126] Y. Wang, A. Liu, Y. Han, and T. Li, “Sensors based on conductive polymers and their composites: a review,” *Polym. Int.*, vol. 69, no. 1, pp. 7–17, 2020.

[127] S. K. Al-Hayali, A. M. Salman, and A. H. Al-Janabi, “High sensitivity balloon-like interferometric optical fiber humidity sensor based on tuning gold nanoparticles coating thickness,” *Measurement*, vol. 170, p. 108703, 2021.

[128] D. I. Al-Janabi, A. M. Salman, and A. H. M. Al-Janabi, “All fiber, highly sensitive sensor based on gold nanoparticle-coated macrobent single mode fiber for human temperature monitoring,” *J. Nanophotonics*, vol. 14, no. 4, p. 46013, 2020.

[129] L. A. Ribeiro *et al.*, “Fiber optic bending loss sensor for application on monitoring of embankment dams,” in *2011 SBMO/IEEE MTT-S International Microwave and Optoelectronics Conference (IMOC*

2011), 2011, pp. 637–641.

[130] J. Eisenstein, P. Y. Wong, and C. G. L. Cao, “Evaluation of techniques to model bend loss in multimode fibers for endoscopic application,” *Appl. Opt.*, vol. 49, no. 12, pp. 2220–2231, 2010.

[131] E. N. Fokoua, M. N. Petrovich, T. Bradley, F. Poletti, D. J. Richardson, and R. Slavík, “How to make the propagation time through an optical fiber fully insensitive to temperature variations,” *Optica*, vol. 4, no. 6, pp. 659–668, 2017.

[132] L. E. Rodríguez-Vilchis, R. Contreras-Bulnes, O. F. Olea-Mejìa, I. Sánchez-Flores, and C. Centeno-Pedraza, “Morphological and structural changes on human dental enamel after Er: YAG laser irradiation: AFM, SEM, and EDS evaluation,” *Photomed. Laser Surg.*, vol. 29, no. 7, pp. 493–500, 2011.

[133] T. S. Al-Qaradaghi, A. S. Mahmood, and R. N. Dayem, “The Efficacy of Er: YAG Laser on Intrapulpal Temperature Rise of Class V Cavity Preparation,” *Iraqi J. Laser*, vol. 10, no. B, pp. 9–14, 2011.

[134] J. Diaci and B. Gaspirc, “Comparison of Er:YAG and Er, Cr:YSGG lasers used in dentistry,” *J. Laser Heal. Accademy*, vol. 2012, no. 1, pp. 1–13, 2012.

[135] M. S. Bello-Silva *et al.*, “Precise ablation of dental hard tissues with ultra-short pulsed lasers. Preliminary exploratory investigation on adequate laser parameters,” *Lasers Med. Sci.*, vol. 28, no. 1, pp. 171–184, 2013.

[136] K. Cantekin, S. K. Buyuk, E. Delikan, K. Pedük, and S. Demirbuga, “Pulp chamber temperature increase from curing light units: an in vitro

study," *J. Dent. Child.*, vol. 81, no. 3, pp. 128–132, 2014.

[137] P. Runnacles *et al.*, "In vivo temperature rise in anesthetized human pulp during exposure to a polywave LED light curing unit," *Dent. Mater.*, vol. 31, no. 5, pp. 505–513, 2015.

[138] L. M. L. Andreatta, A. Y. Furuse, A. Prakki, J. F. S. Bombonatti, and R. F. L. Mondelli, "Pulp chamber heating: an in vitro study evaluating different light sources and resin composite layers," *Braz. Dent. J.*, vol. 27, pp. 675–680, 2016.

[139] C. R. A. C. de Oliveira *et al.*, "Analysis of Human Tooth Pulp Chamber Temperature After 670 nm Laser Irradiation: In Vitro Study," *Photomed. Laser Surg.*, vol. 35, no. 10, pp. 515–519, 2017.

[140] L. Fan, Z. Zou, J. Barsha, X. Liang, and B. Shilu, "Effect of laser treatment of dentin hypersensitivity on pulp chamber temperature," *Int. J. Biomed. Eng.*, vol. 41, no. 2, pp. 172–176, 2018.

[141] I. F. Ra'fat, "Effect of cooling water temperature on the temperature changes in pulp chamber and at handpiece head during high-speed tooth preparation," *Restor. Dent. Endod.*, vol. 44, no. 1, 2019.

[142] K. A. KAMATH and I. NASIM, "Evaluation of laser guided infrared thermometry as an auxiliary tool for pulp vitality assessment-a clinical study.," *Int. J. Pharm. Res.*, vol. 12, no. 4, 2020.

[143] A. Kaushik, R. R. Singh, P. Rani, G. V. Kumar, P. R. S. Khurana, and T. Kaur, "Effect of Three Different Cooling and Insulation Techniques on Pulp Chamber Temperature during Direct Temporization with Polymethyl methacrylate-based Resin," *J. Contemp. Dent. Pract.*, vol. 22, no. 6, pp. 644–649, 2021.

[144] C. de C. A. Lopes, P. H. J. O. Limirio, V. R. Novais, and P. Dechichi, "Fourier transform infrared spectroscopy (FTIR) application chemical characterization of enamel, dentin and bone," *Appl. Spectrosc. Rev.*, vol. 53, no. 9, pp. 747–769, 2018.

[145] L. C. Palmer, C. J. Newcomb, S. R. Kaltz, E. D. Spoerke, and S. I. Stupp, "Biomimetic systems for hydroxyapatite mineralization inspired by bone and enamel," *Chem. Rev.*, vol. 108, no. 11, pp. 4754–4783, 2008.

[146] H. Zhengbing *et al.*, "Data science applications to improve accuracy of thermocouples," in *2016 IEEE 8th International Conference on Intelligent Systems (IS)*, 2016, pp. 180–188.

[147] T. Harashima *et al.*, "Morphological comparative study on ablation of dental hard tissues at cavity preparation by Er: YAG and Er, Cr: YSGG lasers," *Photomed. Laser Ther.*, vol. 23, no. 1, pp. 52–55, 2005.

[148] V. Armengol, A. Jean, and D. Marion, "Temperature rise during Er: YAG and Nd: YAP laser ablation of dentin," *J. Endod.*, vol. 26, no. 3, pp. 138–141, 2000.

[149] H.-C. Lauer, E. Kraft, W. Rothlauf, and T. Zwingers, "Effects of the temperature of cooling water during high-speed and ultrahigh-speed tooth preparation," *J. Prosthet. Dent.*, vol. 63, no. 4, pp. 407–414, 1990.

[150] P. Ottl and H.-C. Lauer, "Temperature response in the pulpal chamber during ultrahigh-speed tooth preparation with diamond burs of different grit," *J. Prosthet. Dent.*, vol. 80, no. 1, pp. 12–19, 1998.

[151] M. Sulieman, J. S. Rees, and M. Addy, "Surface and pulp chamber temperature rises during tooth bleaching using a diode laser: a study in

vitro," *Br. Dent. J.*, vol. 200, no. 11, pp. 631–634, 2006.

[152] A. J. Panas, M. Preiskorn, M. Dąbrowski, and S. Żmuda, "Validation of hard tooth tissue thermal diffusivity measurements applying an infrared camera," *Infrared Phys. Technol.*, vol. 49, no. 3, pp. 302–305, 2007.

[153] M. Sulieman, M. Addy, and J. S. Rees, "Surface and intra-pulpal temperature rises during tooth bleaching: an in vitro study," *Br. Dent. J.*, vol. 199, no. 1, pp. 37–40, 2005.

[154] P. Linsuwanont, J. E. Palamara, and H. H. Messer, "Thermal transfer in extracted incisors during thermal pulp sensitivity testing," *Int. Endod. J.*, vol. 41, no. 3, pp. 204–210, 2008.

[155] M. Preiskorn, S. Zmuda, J. Trykowski, A. Panas, and M. Preiskorn, "In vitro investigations of the heat transfer phenomena in human tooth," *Acta Bioeng. Biomech.*, vol. 5, no. 2, pp. 23–36, 2003.

[156] M. Daronch, F. A. Rueggeberg, G. Hall, and F. Mario, "Effect of composite temperature on in vitro intrapulpal temperature rise," *Dent. Mater.*, vol. 23, no. 10, pp. 1283–1288, 2007.

[157] M. Lin, F. Xu, T. J. Lu, and B. F. Bai, "A review of heat transfer in human tooth—experimental characterization and mathematical modeling," *Dent. Mater.*, vol. 26, no. 6, pp. 501–513, 2010.

[158] Y. Minesaki, "Thermal properties of human teeth and dental cements," *Shika Zair. kikai= J. Japanese Soc. Dent. Mater. Devices*, vol. 9, no. 4, pp. 633–646, 1990.

[159] J. K. Carson, S. J. Lovatt, D. J. Tanner, and A. C. Cleland, "Thermal conductivity bounds for isotropic, porous materials," *Int. J. Heat Mass Transf.*, vol. 48, no. 11, pp. 2150–2158, 2005.

[160] A. POHTO, M.; SCHEININ, “Microscopic observations on living dental pulp.,” *Acta Odontol. Scand.*, vol. 16, pp. 303–327, 1958.

[161] K. Kodonas, C. Gogos, and C. Tziafa, “Effect of simulated pulpal microcirculation on intrachamber temperature changes following application of various curing units on tooth surface,” *J. Dent.*, vol. 37, no. 6, pp. 485–490, 2009, doi: 10.1016/j.jdent.2009.03.006.

[162] R. Hibst and U. Keller, “Heat effect of pulsed Er: YAG laser radiation,” in *Laser Surgery: Advanced Characterization, Therapeutics, and Systems II*, 1990, vol. 1200, pp. 379–386.

[163] U. Keller and R. Hibst, “Ultrastructural changes of enamel and dentin following Er: YAG laser radiation on teeth,” in *Laser Surgery: Advanced Characterization, Therapeutics, and Systems II*, 1990, vol. 1200, pp. 408–415.

[164] K. Baroudi, N. Silikas, and D. C. Watts, “In vitro pulp chamber temperature rise from irradiation and exotherm of flowable composites,” *Int. J. Paediatr. Dent.*, vol. 19, no. 1, pp. 48–54, 2009.

Publications

The following publication prior to this thesis:

- **Highly efficient optical fiber sensor for instantaneous measurement of elevated temperature in dental hard tissues irradiated with an Nd:YaG laser.**

applied optics, OSA journal, 16 July 2021, published.

Authors: Zahraa J. Naeem, Ansam M. Salman, Rawaa A. Faris, and Abdulhadi Al-Janabi.

Q ranking of journal: Q1.

Index: Clarivate Analysis and Scopus.

https://doi.org/10.1364/AO.431369

Research Article Vol. 60, No. 21 / 20 July 2021 / Applied Optics 6189

applied optics

Highly efficient optical fiber sensor for instantaneous measurement of elevated temperature in dental hard tissues irradiated with an Nd:YaG laser

Zahraa J. Naeem,[1,*] Ansam M. Salman,[1,2] Rawaa A. Faris,[1] and Abdulhadi Al-Janabi[1]

[1]Institute of Laser for Postgraduate Studies, University of Baghdad, Baghdad, Iraq
[2]Laser and Optoelectronics Department, College of Engineering, Al-Nahrain University, Baghdad, Iraq
*Corresponding author: zahraaj333@gmail.com

Received 14 May 2021; revised 9 June 2021; accepted 16 June 2021; posted 17 June 2021 (Doc. ID 431369); published 16 July 2021

In this *in vitro* experiment, the effect of 1.064 µm pulsed laser on both enamel- and dentin-dental tissues has been investigated. A total of fifty-five dental hard tissue samples were exposed to Nd:YAG laser that possesses a pulse width of 9 ns and 850 mJ of total energy. An optical fiber sensor was put behind the samples to measure the temperature instantaneously. A novel, to the best of our knowledge, fiber sensor has been proposed and used to measure the heat generated in dental hard tissues instantaneously after the application of laser irradiation on the tissue surface. This optical sensor exhibits a fast response time of about 1 ms and high sensitivity with about 1.975 nm/°C. The findings of this study in decreasing the probability of pulpal necrosis structure while handling the tooth, whether for ablation, welding, or tooth resurfacing purposes, may establish standards for dentists and laser manufacturers (healthcare professionals) that should be followed.

https://doi.org/10.1364/AO.431369

1. INTRODUCTION

In recent decades, laser clinical utilization for dental hard tissue treatment has become an actuality. The laser technique is used for several dental treatment processes in the oral cavity including frenectomy, gingivectomy, and soft tissue surgical excisions or incisions, in addition to a range of periodontal procedures for soft oral tissues [1,2]. For several years, research on therapeutic lasers in the dental zone have been carried out to study the potential and appropriateness of laser techniques and their variables to replace the conventional process. The results of the therapeutic laser rely on both the physical features of the tissue material as well as the laser radiation parameters [3]. So accurate observance has to be achieved by choosing parameter settings, laser types, wavelength, pulse width, energy, and optical features of the target tissue including the absorption as well as scattering influence [4,5]. A lot of researchers are interested in laser ablation of hard tissue for cavity production as it is supposed to be beneficial, lessens discomfort, and provides patients with more relaxed care by dramatically reducing noise and vibrations compared to conventional burs [6–11]. The term "laser ablation" is defined by means of the substance elimination/removal from the objective tissue through heating by laser.

Heat production through the elimination of oral dental hard tissues results in temperature rise and trigger aching senses or injure oral dental tissues. *In vivo* study of heat-exposed dental pulps showed that a rise in temperature to 39°C–42°C leads to increase circulation (hyperemia) [12]. Thrombosis and a standstill in circulation occurred when temperatures of 46°C–50°C are sustained for a few seconds. *In vivo* research compared the increase in tooth surface temperature with an internal elevation in temperature [13]. A rise to 42.2°C in the pulpal temperature could be seen to contribute to pulpal death that has been found in some instances, and an additional increase in the temperature in their animal model lead to more than half of the teeth having necrosis. As a result, to prevent unintended side effects, it is necessary to determine the potential heat production ability for every new tooth preparation technique. The efficacy of the heating and its magnitude are mainly governed by two practices: the absorption of the laser energy and heat reorganization owing to heat conductivity. These factors decide laser tissue heating temperature and tissues heating depth in the exposed region and then the degree of material elimination and the threshold of the ablation (the smallest value of laser energy that regards etching of the tissue). In general, the principal challenge for the target under study remains choosing the parameters of the laser for good ablation [3,14,15]. Even though there has also been development in decreasing the occurrence of dental caries, dental decay remains an important health difficulty, and

1559-128X/21/216189-10 Journal © 2021 Optical Society of America

وزارة التعليم العالي والبحث العلمي

جامعة بغداد

معهد الليزر للدراسات العليا

متحسس الليف البصري السريع لاستشعار زيادة درجة الحرارة أثناء تحضير التجويف السني بالليزر

رسالة مقدمة الى

معهد الليزر للدراسات العليا /جامعة بغداد /لاستكمال متطلبات نيل شهادة ماجستير علوم في الليزر/ طب الاسنان

من قبل

زهراء جابر نعيم

بكالوريوس طب وجراحة الفم والاسنان

بأشراف

الأستاذ الدكتور عبد الهادي مطشر الجنابي

١٤٤٢هـ **٢٠٢١ م**

الخلاصة

الهدف: يمكن أن يحدث ارتفاع في درجة الحرارة نتيجة لتراكم الحرارة أثناء تحضير تجويف أنسجة الأسنان الصلبة باستخدام شعاع الليزر. يتم تطبيق طريقة قياس مبتكرة تعتمد على مستشعر الألياف للقياس الفوري لارتفاع الحرارة في أنسجة الأسنان الصلبة المينا والعاج. تم اختبار تأثير ليزر

بطول موجة Er ،Cr: YSGG بطول موجة ١٠٦٤ نانومتر وكذلك Nd: YAGتم اختبار تأثير ليزر ٢٧٨٠ نانومتر على أنسجة الأسنان المينا والعاج.

المواد والطرق: تم تحضير ١١٠ عينة من الأنسجة الصلبة للأسنان مأخوذة من كل من المينا وعاج الأسنان ذات سماكة طبقة مختلفة. تم اختبار تأثير كل من أطوال موجات الليزر المذكورة أعلاه من حيث التأثير السلبي الحراري على لب الأسنان أثناء تحضير تجويف الليزر. أولاً، تم علاج نصف هذه الأنسجة الصلبة للأسنان باستخدام الليزر القريب من الأشعة تحت الحمراء Q-switched Nd: YAG (λ = 1.06 ميكرومتر) لمدة نبضة ٩ نانوثانية، ومعدل تكرار ١٠ هرتز، وإجمالي طاقة ٨٥٠ مللي جول ومتوسط بقوة ٨,٥ وات تقريبًا تم تشعيع هذه العينات باستخدام معجون موصل للحرارة كوسيط واجهة بدون أي تبريد أو رش ماء. بعد ذلك، تم التحقق من تأثير ليزر Er ،Cr: YSGG (λ = 2.7 ميكرومتر) مع مدة نبضة ٦٠ ميكرو ثانية ، وطاقة ٢٦٠ مللي جول ، ومعدل تكرار ١٥ هرتز ، وقطر طرف ليفي ٦٠٠ ميكرومتر وقوة ٤ وات. بمعدل ٥٠٪ ماء و ٨٠٪ رذاذ هواء.

لقياس ارتفاع درجة الحرارة بشكل فوري وسريع، تم تصميم وإنشاء مستشعر ألياف بصرية جديد مع شكل يشبه البالون. يعتمد مستشعر الألياف الضوئية سهل التكيف والمعلق على الجزء الخلفي من عينات المينا والعاج على مبدأ مقياس التداخل Mach-Zehnder. يمتلك المستشعر أعلاه، الذي تم استخدامه، وقت استجابة سريعًا يبلغ حوالي ١ مللي ثانية، ووقت استرداد سريع يبلغ ٢,٧٣ مللي ثانية، فضلاً عن مقاومة عالية عند حوالي ١,٩٧٥ نانومتر / ٠ درجة مئوية.

النتائج: تم استخدام نوعين مختلفين من الليزر (Nd: YAG وEr,Cr:YSGG) لإجراء التجارب في المختبر. نظرًا لأن الحد الآمن لحيوية اللب سيحدد معلمات الليزر المستخدمة، أظهر تحضير تجويف ليزر Nd: YAG بدون تبريد بالماء ارتفاعًا في درجة الحرارة أعلى منEr,Cr:YSGG في ثلاث مجموعات فرعية (المينا ١ مم ، المينا ٢ مم وسمك المينا ٢ مم). بينما لوحظت أدنى قيم درجات الحرارة في المجموعة الفرعية (العاج ٣ مم).

ومع ذلك، تم التحكم في حزم الليزر المطبقة بالكامل لتجنب ارتفاع درجة الحرارة غير المرغوب فيه عبر مستشعر الألياف الضوئية المستخدم. بفضل خصائصه الفريدة من نوعها، يساعد المستشعر كثيرًا في إعطاء استجابة مفيدة في الوقت المناسب للحفاظ على حيوية اللب.

الاستنتاجات: الجمع بين الليزر عالي الكفاءة لتحضير التجاويف ووقت الاستجابة السريع، وسيوفر مستشعر الألياف المتكيف بسهولة منصة محتملة لتجنب نخر اللب من خلال عملية استئصال الأسنان بالليزر.